

Multimodal Medical Image Fusion: Techniques, Databases, Evaluation Metrics, and Clinical Applications -A Comprehensive Review



Nidhi Goswami¹, Ayush Dogra^{2,*}, Sonika Bakshi¹ and Bhawna Goyal³

¹Chitkara School of Health Sciences, Chitkara University, Rajpura, Punjab, India

²Chitkara University Institute of Engineering and Technology, Chitkara University, Rajpura, Punjab, India

³Department of Engineering, Marwadi University Research Centre, Marwadi University, Rajkot, Gujarat, India

Abstract:

Multi-modal Medical Image Fusion (MMIF) is an advancing field at the intersection of medical imaging, data science, and clinical diagnostics. It aims to integrate complementary data from various imaging modalities, such as MRI, CT, and PET, into a single, diagnostically superior composite image. The limitations of unimodal imaging, such as low spatial resolution, insufficient contrast, or incomplete functional characterization, have catalyzed the development of MMIF techniques to enable enhanced visualization, precise diagnosis, and personalized therapeutic planning. This review provides a comprehensive synthesis of the MMIF landscape, categorizing methodologies into five principal domains such as spatial, frequency-based, sparse representation, deep learning, and hybrid approaches. Each technique is critically evaluated for its advantages, limitations, and applicability in clinical settings. Preprocessing, registration, fusion execution, and validation are covered in this review, along with levels of fusion pixel, feature, and decision. The study reviews prominent public databases, including TCIA, OASIS, ADNI, MIDAS, AANLIB, and DDSM, comparing their imaging modalities, disease coverage, file formats, and accessibility. The evaluation of MMIF techniques is systematically addressed, providing a framework for objective performance assessment. An experimental setup is implemented on two datasets to assess the comparative efficacy of selected MMIF techniques utilizing quantitative evaluation variables such as SSIM, entropy, spatial frequency, and mutual information. The results highlight the effectiveness of hybrid and deep learning-based approaches in maintaining both anatomical detail and functional consistency across modalities. The review explores MMIF's real-world clinical applications, including image-guided neurosurgery, spinal planning, stereotactic radiosurgery, orthopedic implant design, and oncology diagnostics. It also provides insights into future directions, such as explainable AI, federated learning, and integration with robotic surgeries. MMIF offers immense potential yet has limitations like registration errors, computational burdens, generation of artifacts, loss of specific information, and a lack of standardized evaluation metrics. Essentially, the study provides an analytical basis for healthcare experts, scientists, and engineers aiming to develop clinically scalable MMIF systems, which will become indispensable tools for improving diagnostic accuracy, treatment planning, and patient outcomes in modern healthcare.

Keywords: Multimodal medical image fusion, Spatial, Deep learning, Sparse representation, Transform, Hybrid fusion techniques.

© 2025 The Author(s). Published by Bentham Open.

This is an open access article distributed under the terms of the Creative Commons Attribution 4.0 International Public License (CC-BY 4.0), a copy of which is available at: <https://creativecommons.org/licenses/by/4.0/legalcode>. This license permits unrestricted use, distribution, and reproduction in any medium, provided the original author and source are credited.

*Address correspondence to this author at the Chitkara University Institute of Engineering and Technology, Chitkara University, Rajpura, Punjab, India; E-mail: ayush123456789@gmail.com

Cite as: Goswami N, Dogra A, Bakshi S, Goyal B. Multimodal Medical Image Fusion: Techniques, Databases, Evaluation Metrics, and Clinical Applications -A Comprehensive Review. Open Neuroimaging J, 2025; 18: e18744400417835. <http://dx.doi.org/10.2174/0118744400417835251022042920>



CrossMark

Received: June 11, 2025

Revised: July 09, 2025

Accepted: July 15, 2025

Published: November 11, 2025



Send Orders for Reprints to
reprints@benthamscience.net

1. INTRODUCTION

Medical imaging is an essential part of clinical diagnostics because it allows physicians to visualize and evaluate anatomical and physiological structures without surgical intervention. Single imaging approaches are often insufficient to capture all the necessary details, especially when both anatomical and functional aspects need to be evaluated. Magnetic Resonance Imaging (MRI) is known for its high soft tissue resolution but lacks biochemical data detection, whereas Positron Emission Tomography (PET) provides functional metabolic information at the expense of structural precision. Due to these constraints, research has grown significantly in this field. MMIF is defined as the combination of complementary information from various imaging modalities for image enhancement, accuracy, and interpretation. For quality assurance, the fused image should not deviate from the essential characteristic of the input modalities involved and should not be distorted, occluded, or stained with artefacts [1]. For example, combining PET and MR data allows for a detailed depiction of both the anatomy of soft tissues and functional tumor metabolism, which is crucial for oncology and neuroimaging. The use of CT and MRI fusion, as shown in Fig. (1), allows clinicians to have a clear overall overview of the bone structures and soft tissue during treatment planning for radiotherapy and guidance for complex surgical navigations.

The development in the field of medical technology, along with the increasing diversity of medical conditions, substantiates the crucial role of multimodal image fusion. The rise in chronic illnesses makes multimodal imaging a

treasured means of understanding the progression of the disease. Despite its merits, there are many challenges for MMIF. The fusion method must accurately preserve the spatial, spectral, and contrast characteristics of the source images. The choice of techniques for co-registration should be proper because images from different modalities, such as PET and MRI, must register precisely, considering the size, resolution, and noise differences [2].

The fusion approaches are categorized into three levels: pixel, feature, and decision, which aim to generate a fused image that enhances visual perception. Traditional medical image fusion techniques are categorized into spatial, transform, and hybrid. The radical change in the automation and performance of methods in MMIF has been fueled by the use of convolutional neural networks, autoencoders, and attention-based architectures [3]. Data-driven learning enables these models to create mature fusion strategies that are more adaptive and generalizable than conventional rule-based models. The application of transformer-based models and GANs has demonstrated positive results for MMIF operations, particularly in PET-MRI fusion and creation of high-resolution medical images [4]. Applications for MMIF include the localization of brain tumors, identifying breast cancer, as well as assessing bone fractures and cardiovascular health. Fused images are also helpful for Computer-Aided Diagnosis (CAD) systems, which, after inputting multimodal data, can generate models that, in turn, increase diagnostic accuracy. Besides, MMIF allows enhanced presentation of key structures and lesions, which are useful in pre-surgical planning, radiotherapy, and interventional procedures [5].

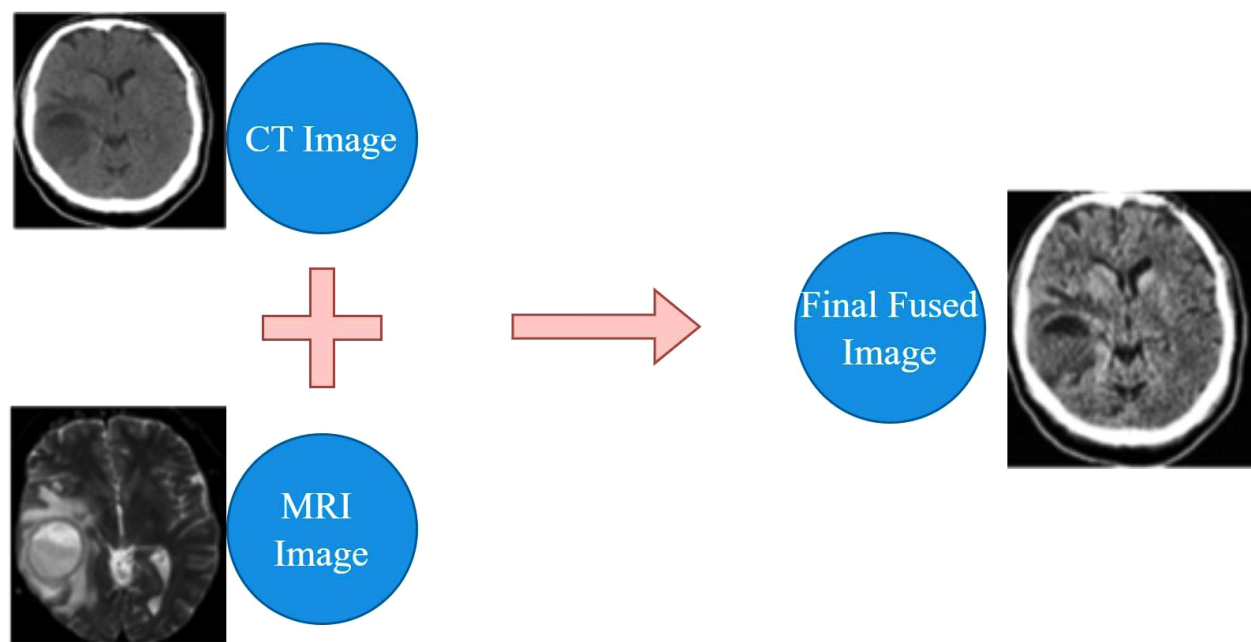


Fig. (1). Medical image fusion [2].

This review aims to provide comprehensive information on the multimodal medical image fusion field, encompassing traditional techniques, recent advances, and future trends. The various sections of the review are organized under the following headings.

- 1. A comparison of major medical imaging modalities.
- 2. An overview of publicly available multimodal medical image databases, including TCIA, OASIS, ADNI, MIDAS, and AANLIB.
- 3. MMIF steps: preprocessing, registration, fusion strategy, and performance evaluation.
- 4. A taxonomy of fusion techniques.
- 5. Applications of Image Fusion in Clinical Medicine.
- 6. Image Quality Metrics in Medical Image Fusion.

- 7. Experimental Set Up and Discussion.
- 8. Challenges in MMIF deployment.
- 9. Emerging trends and future directions.

Through this review, we aim to lay a foundational understanding that not only serves current practitioners but also guides future research in designing clinically relevant and scalable MMIF solutions. A comparative analysis of recent review papers on MMIF, emphasizing key criteria such as modality presentation, domain categorization, database accessibility, quantitative evaluation, and clinical applications, is done in Table 1. Figure 2a depicts the growth in publications in this field, and Figure 2b shows the process followed for literature review from 2014 to 2024.

Table 1. Comparative overview of recent review studies on multimodal image fusion.

Review (Year of Publication)	Presentation of Modalities for Imaging	Presented Domains of MMIF	Publicly Accessible Databases	Quantitative Evaluation Results	Key Challenges and Future Directions	Clinical Applications
Tirupal <i>et al.</i> , 2021 [8]	Yes	Yes	No	Yes	Yes	No
Hermessi <i>et al.</i> , 2021 [59]	Yes	Yes	No	Yes	Yes	No
Haribabu <i>et al.</i> 2022 [5]	Yes	Yes	No	Yes	No	No
Saleh <i>et al.</i> 2023 [6]	Yes	Yes	No	Yes	No	No
Diwakar <i>et al.</i> 2023 [52]	Yes	Yes	No	Yes	Yes	No
Kalamkar and Mary 2023 [2]	Yes	Yes	No	No	Yes	No
Khan <i>et al.</i> , 2023 [19]	Yes	Yes	Yes	Yes	Yes	No
Our Work	Yes	Yes	Yes	Yes	Yes	Yes

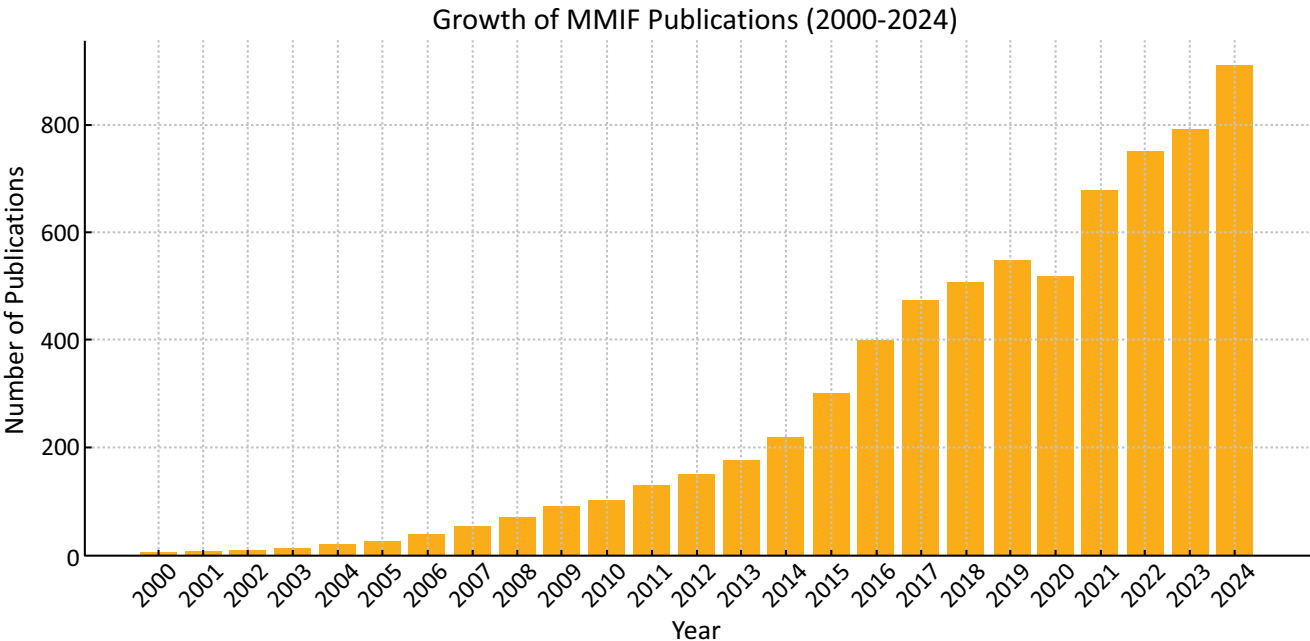


Fig. (2a). Growth in MMIF publication trend chart (WOS).

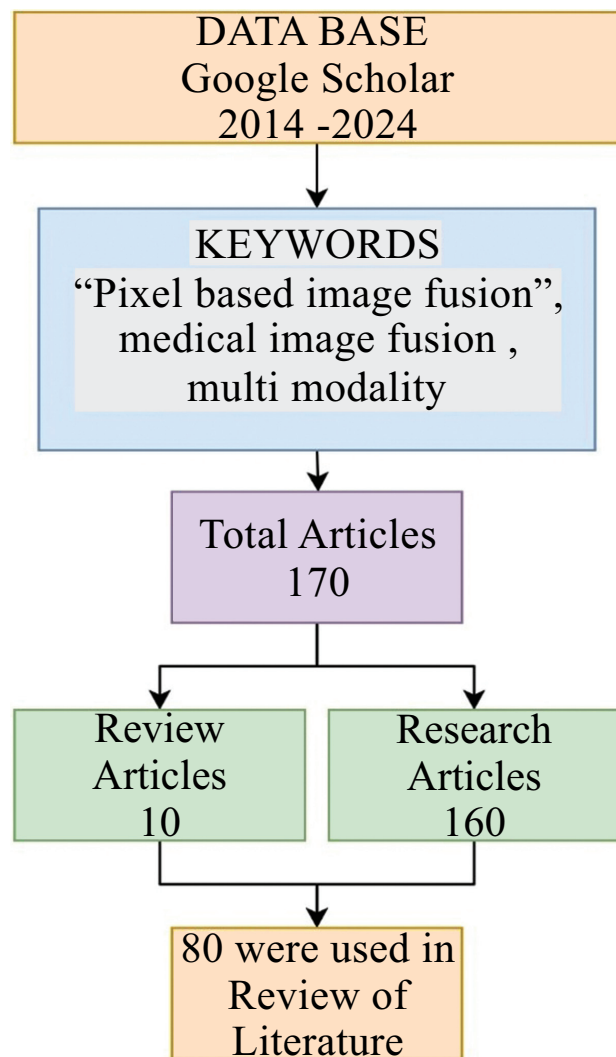


Fig. (2b). Flowchart illustrating the article selection process for a literature review on pixel-based image fusion in medical imaging, covering publications from 2014 to 2024.

The methodology adopted for this study involved a structured literature search and screening process from 2014–2024. Google Scholar was selected as the principal database due to its comprehensive indexing of scholarly articles across several disciplines, ensuring the inclusion of the most relevant and recent advancements in the field. Specific keywords such as “Pixel-based image fusion,” “medical image fusion,” and “multi-modality” were used. This initial search yielded a total of 170 articles. These were then categorized into review articles (10) and research articles (160) based on their scope and content. The selection process emphasized relevance to the research objectives, specifically focusing on pixel-level fusion methods and their applications in medical imaging. Articles not related to the scope, duplicates, or those with insufficient methodological details were excluded. After

this screening, 80 articles were finalized and critically analyzed for the literature review under five different domains, *i.e.*, spatial, transform, deep learning, sparse, and hybrid.

1.1. Imaging Modalities in Medical Image Fusion

Through the fusion of several medical imaging techniques, MMIF manages to gather a variety of information concerning structural and functional features of human bodies. An overview of structural, functional, and multimodal imaging modalities is given in Fig. (3).

X-rays are a fundamental imaging modality and are still highly used for imaging bones, for identifying fractures, infections, tumors, *etc.*, in a two-dimensional image. Computed Tomography (CT) is a method that utilizes ionizing radiation in the form of X-rays for producing cross-sectional three-dimensional images of the body in great detail. It is superior in visualizing bones, revealing internal bleeding, and detecting tumors. CT scans offer rapid and cost-effective imaging, making them a routine choice in trauma evaluations; however, they involve exposure to ionizing radiation [6]. While CT excels in imaging bones compared to MRI, it cannot differentiate soft tissues as effectively.

Magnetic Resonance Imaging (MRI) is a non-invasive technology that uses magnetic fields and radio waves to create high-quality images of soft tissues in the brain, muscles, and other internal organs without the use of ionizing radiation. Owing to its superior image quality and the absence of radiation exposure, MRI is the modality of choice for evaluating brain tumors, spinal cord abnormalities, and ligament injuries [7].

Positron Emission Tomography (PET) is an invasive imaging modality utilizing ionizing radiation to assess metabolic and functional processes within the body. The technique involves administering a radiotracer that emits positrons during radioactive decay. PET is beneficial for oncology, neurology, and cardiology because it detects biochemical changes before anatomical changes are observable. The PET’s weak spatial resolution is complemented by its combination with MRI or CT techniques to enhance anatomical mapping. SPECT and PET use radioactive tracers to measure blood flow and metabolic processes. However, SPECT has less sensitivity and poorer imaging resolution than PET. Despite its limitations, SPECT offers important data for diagnosing cardiac perfusion problems, epilepsy, and bone disorders. When SPECT is combined with CT or MRI, its diagnostic reliability increases significantly, minimizing the effect of its poorer spatial resolution. fMRI uses the measurement of changes in blood oxygenation and flow that correspond to neural activity as an extension of a standard MRI. It is especially evident in brain mapping applications in neuroscience research and surgery planning. Researchers at MMIF often combine fMRI with structural MRI to impart brain function to particular anatomical structures [8]. Table 2 presents the categorization of imaging modalities, such as ultrasound and endoscopy, according to their degree of invasiveness and the extent of patient exposure to ionizing radiation.

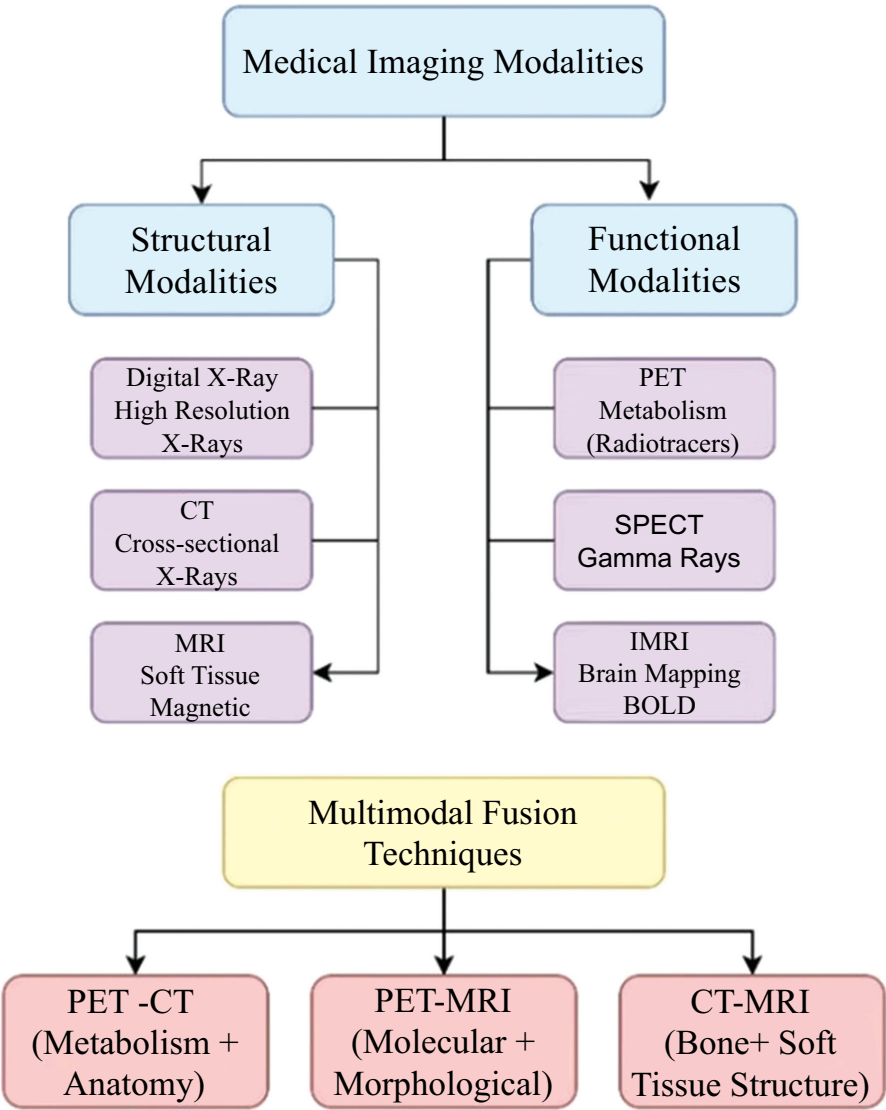


Fig. (3). Overview of structural, functional, and multimodal medical imaging modalities.

Table 2. Comparative analysis of medical imaging modalities.

Modality	Type of Information	Invasiveness	Ionizing Radiation	Resolution	Typical Use Cases
MRI	Anatomical (soft tissue)	Non-invasive	No	High spatial	Brain, spinal cord, joints
CT	Anatomical (bone/soft tissue)	Non-invasive	Yes	High spatial	Trauma, tumors, lungs
PET	Functional (metabolic)	Slightly Invasive (radiotracer)	Yes	Low spatial	Cancer staging, brain disorders
SPECT	Functional (blood flow)	Slightly Invasive (radiotracer)	Yes	Low spatial	Cardiology, brain perfusion
Ultrasound	Anatomical (real-time soft tissue)	Non-invasive	No	Moderate spatial	Pregnancy, abdomen, heart valves
X-ray	Anatomical (bone, dense tissue)	Non-invasive	Yes	Moderate spatial	Fractures, chest infections
fMRI	Functional (neural activity)	Non-invasive	No	Moderate spatial	Brain mapping
Endoscopy	Visual (surface/internal tissues)	Invasive	No	Very high visual	GI tract visualization, surgical guidance

2. MULTIMODAL MEDICAL IMAGE DATABASES

The development and validation of Multimodal Medical Image Fusion (MMIF) algorithms require robust, diverse, and accessible imaging datasets. Publicly available datasets offer researchers an opportunity to test their fusion methods across multiple imaging modalities and pathological conditions in a reproducible manner. A variety of high-quality databases have emerged in recent years, as shown in Fig. (4), supporting fusion research across neuroimaging, oncology, cardiology, and more. This section highlights some of the most widely used datasets, TCIA, OASIS, ADNI, MIDAS, AANLIB, and DDSM, and outlines their characteristics, disease focus, modality support, and accessibility.

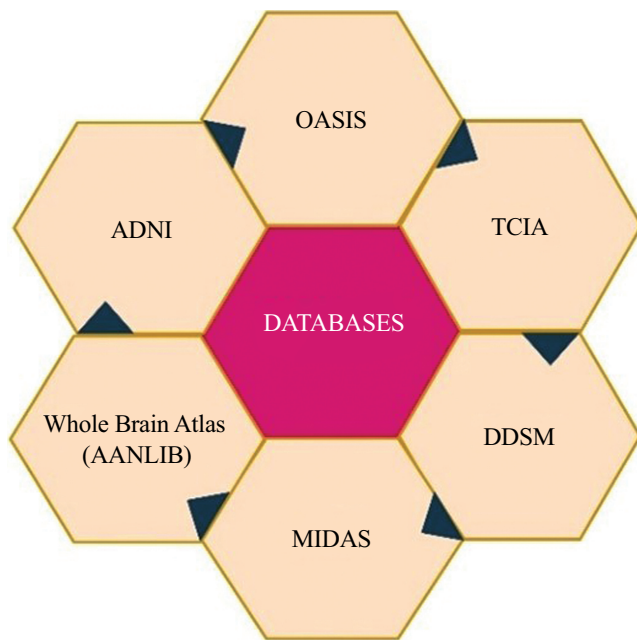


Fig. (4). Major publicly available multimodal medical image databases.

2.1. The Cancer Imaging Archive (TCIA)

TCIA appears to be one of the top sources of comprehensive and exhaustively curated cancer imaging data repositories. Under the direction of the National Cancer Institute (NCI), the collection encompasses more than 50,000 richly varied imaging cases CT, MRI, PET, and histopathology. TCIA is a benchmark for assessing fusion algorithms because of its ability to support multimodal imaging research. For example, the Lung-PET-CT-Dx dataset contains synchronized PET and CT scans for the diagnosis of lung cancer, and BraTS contains multimodal MRI (T1, T1-Gd, T2, FLAIR) images annotated for brain tumor research. The platform allows for direct visualization and annotation support through integration with 3D Slicer, ITK-SNAP [9].

2.2. Open Access Series of Imaging Studies (OASIS)

OASIS provides an extensive collection of neuroimaging data, specifically, destined for studies in aging, Alzheimer's disease, and cognitive deficits. OASIS consists of cross-sectional MRI and PET imaging datasets. OASIS-3, the latest version, contains over 2,000 subjects that had a series of imaging sessions, genetic testing, and clinical testing [10]. The variety of modalities within OASIS datasets makes them ideal for fusion studies. One example is the accuracy of diagnosis of Alzheimer's disease at its earliest stages by using the amyloid PET along with the T1-weighted MRI. Each dataset is represented in the NIfTI format, a reputable neuroimaging standard, and is accompanied by metadata that includes the results of cognitive evaluations.

2.3. Alzheimer's Disease Neuroimaging Initiative (ADNI)

ADNI is a collaborative investigation for the study of the progress of Alzheimer's disease through imaging and clinical data. It provides rich longitudinal data drawn from several imaging and biomarker modalities such as MRI, FDG-PET, amyloid PET, and CSF biomarkers. The initiative tracks more than 1,700 participants through various stages of cognitive decline. ADNI research subjects are characterized at three cognitive levels such as cognitively normal, MCI, and Alzheimer's disease. The large temporal resolution of ADNI allows the study of temporal dynamics of brain change represented by other imaging technologies. In many ADNI data-based investigations, researchers use fusion methods to predict progression from MCI to Alzheimer's by combining structural MRI with metabolic PET information [11]. Researchers can obtain data from the ADNI through an application process, in the form of DICOM and NIfTI, via the Laboratory of Neuro Imaging (LONI) platform.

2.4. Medical Image Data Archive System (MIDAS)

MIDAS, an adaptable data management system, was developed by Kitware, which serves the area of imaging datasets, including the realms of radiology, pathology, and ultrasound. The system's flexible architecture enables the integration and storage of 2D and 3D imaging data together with corresponding clinical and demographic records. The uniqueness of MIDAS is its capability to integrate custom plugins and tools, which is useful for researchers who work with end-to-end pipelines for image fusion and segmentation. Some of the commonly used datasets in MMIF research include Head-Neck Cancer CT-MRI and Cardiac MR + Ultrasound [12]. MIDAS can handle DICOM, RAW, and MetaImage (.mha).

2.5. Digital Database for Screening Mammography (DDSM)

The DDSM repository exists with the objective of large-scale breast detection, predominantly facilitated by X-ray mammograms. Although the repository originally concentrated on one modality, the recent additions, such as INbreast and CBIS-DDSM, have included histopathology

and ultrasound data for supporting multimodal analysis. The DDSM collection contains more than 2,500 studies, several of which are annotated with information about mass boundaries. The DDSM's usefulness for MMIF lies in its synthesis of mammographic features with pathological confirmation, supporting the integration of image and diagnostic data [13].

2.6. Annotated Alzheimer Neuroimaging Library (AANLIB)

AANLIB was created as a dataset specific to assisting multimodal fusion and classification research for Alzheimer's disease. It includes thousands of cases with T1-MRI, FLAIR, PET, and neurocognitive records. Unlike large datasets such as OASIS or ADNI, AANLIB provides images that are prepared for fusion (preprocessing corrects for skull stripping and registration). These standardized images significantly streamline the work in the MMIF workflows. The AANLIB's corresponding images are archived in NIfTI format, and its accompanying ground truth labels are provided for employing it in supervised learning procedures. The open access for academic users makes it suitable for evaluating deep learning fusion algorithms [14]. The source images of the brain from AANLIB in axial, sagittal, and coronal sections are presented in Fig. (5).

2.7. Dataset Summary and Usage Patterns

The most widely used fusion modalities across these datasets include MRI+PET, MRI+CT, and PET+CT,

reflecting the clinical demand for combining anatomical and functional insights. For example, ADNI and OASIS predominantly use MRI+PET, while TCIA and MIDAS offer CT+PET or MRI+CT combinations. Table 3 provides an overview of the available databases with respect to imaging modalities, anatomical regions, and file formats. Regarding disease focus, the datasets are primarily oriented toward the following pathological conditions:

- **Neurodegenerative diseases:** OASIS, ADNI, AANLIB
- **Cancer imaging:** TCIA, DDSM, MIDAS
- **Cardiac and head-neck imaging:** MIDAS
- **Neurofunctional tasks:** AANLIB, OASIS

3. MMIF PROCESS FLOW AND FUSION LEVELS

Multimodal Medical Image Fusion (MMIF) is a complex, multistage process designed to integrate complementary information from multiple imaging modalities into a single, more informative representation. This process is typically divided into four primary stages such as preprocessing, registration, fusion, and validation. Each stage involves distinct technical considerations and affects the overall quality and clinical reliability of the fused output. Furthermore, fusion can be performed at different abstraction levels, pixel, feature, and decision, each offering specific benefits and trade-offs. Understanding this full workflow is critical for designing and evaluating robust MMIF systems.

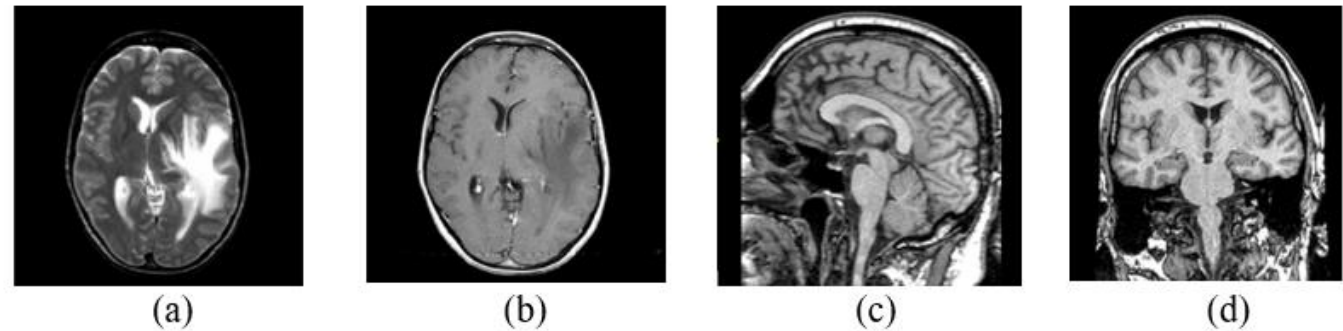


Fig. (5). AANLIB Source images of the brain in axial (a) and (b), sagittal (c), and coronal sections (d) [14].

Table 3. Database summary of modalities, organs, format, and types of access.

Database	Modalities	Target Organs / Systems	File Formats	Access Type
TCIA	CT, MRI, PET, Histopathology	Brain, Lung, Breast, Prostate	DICOM, NIfTI	Open (via API & GUI)
ADNI	MRI, PET, CSF	Brain (Neurodegeneration)	DICOM, NIfTI	Request-based (LONI access)
OASIS	MRI, PET	Brain (Aging, Dementia)	NIfTI	Open (with Data Use Agreement)
AANLIB	MRI, PET, FLAIR	Brain (Alzheimer's)	NIfTI	Open (Academic Use)
MIDAS	CT, MRI, Ultrasound	Head & Neck, Heart, Abdomen	DICOM, MHA, RAW	Open (Kitware tools)
DDSM	Mammography, Histopathology	Breast	LJPEG, DICOM	Open (Preprocessing scripts available)

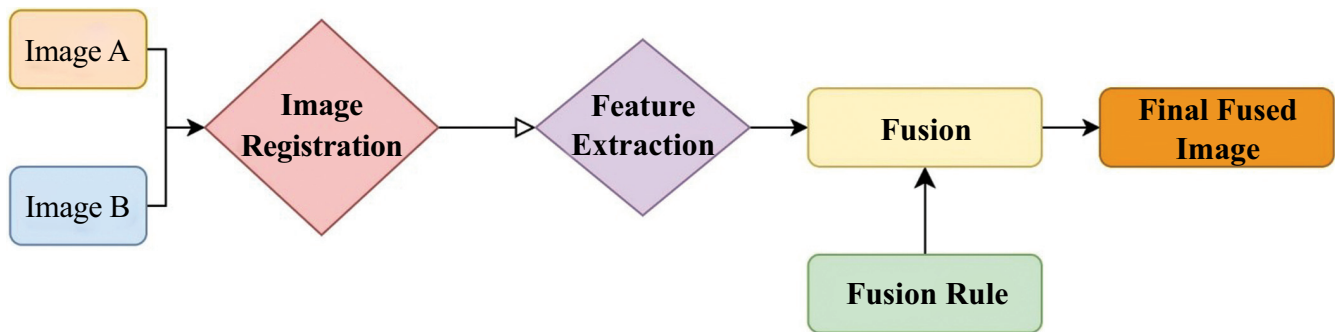


Fig. (6). Steps in the process of image fusion [15].

3.1. Preprocessing

Preprocessing serves as the foundation of MMIF and involves preparing images for further stages by enhancing quality and ensuring uniformity across modalities. This stage includes noise reduction, intensity normalization, contrast enhancement, resolution adjustment, and format conversion. Since different imaging modalities have different spatial resolutions, acquisition angles, and noise characteristics, preprocessing plays a vital role in aligning these disparities. For instance, Magnetic Resonance Imaging (MRI) often exhibits inhomogeneous intensity, while Computed Tomography (CT) is prone to beam-hardening artifacts. Normalizing these differences using histogram equalization or z-score normalization improves the effectiveness of subsequent fusion steps. Additionally, many public datasets like AANLIB provide preprocessed images, including skull stripping and spatial standardization, reducing the preprocessing burden on researchers [15]. Advanced preprocessing techniques such as total variation filtering, anisotropic diffusion, and rolling guidance filters have been adopted in recent MMIF research to preserve structural details while eliminating noise. These techniques are especially beneficial in fusion scenarios involving low-quality or low-contrast images. The process of image fusion is shown in Fig. (6).

3.2. Image Registration

Registration is the process of spatially aligning two or more images of the same anatomical region, but from different modalities. It compensates for differences in image scale, orientation, and position, ensuring that corresponding anatomical structures overlap accurately. The accuracy of registration directly affects the fidelity of the final fused image, especially in pixel- and feature-level fusion.

Image registration methods are typically categorized into rigid, affine, and non-rigid (deformable) techniques. Rigid registration handles only translation and rotation, while affine registration includes scaling and shearing. Non-rigid registration addresses complex deformations and is often necessary when fusing modalities like PET

and MRI due to organ motion or different acquisition geometries. Techniques such as mutual information maximization, normalized cross-correlation, and landmark-based mapping are commonly employed. Deep learning-based registration models, especially U-Net architectures trained on spatial transformer networks, are gaining popularity due to their speed and robustness. These methods can perform unsupervised, real-time registration even in challenging clinical settings.

3.3. Image Fusion Techniques

The core of MMIF is the fusion process itself, which combines information from registered images into a single image. Fusion techniques are classified based on the level at which integration occurs, as described in Fig. (7).

3.3.1. Pixel-level Fusion

Pixel-level fusion is the most straightforward approach, where corresponding pixels from the source images are directly combined using arithmetic or logical operations. Common methods include weighted averaging, maximum selection, and wavelet-based combination. These methods are computationally efficient but highly sensitive to registration errors and noise. Recent enhancements at this level involve multiscale transforms such as NSCT (Non-subsampled Contourlet Transform), DWT, and shearlet transforms, which improve spatial-frequency localization and reduce artifacts [16].

3.3.2. Feature-level Fusion

Feature-level fusion focuses on processing and integrating visual features that are more relevant than individual pixels. This strategy involves independently extracting high-level characteristics such as edges, textures, and shapes from the source images and then using a fusion method on them. This level offers better robustness against misregistration and provides more semantically meaningful outputs, leading to enhanced visual perception, decision-making precision. Techniques like SIFT (Scale-Invariant Feature Transform), Gabor filters, and gradient domain methods are widely used for this purpose.

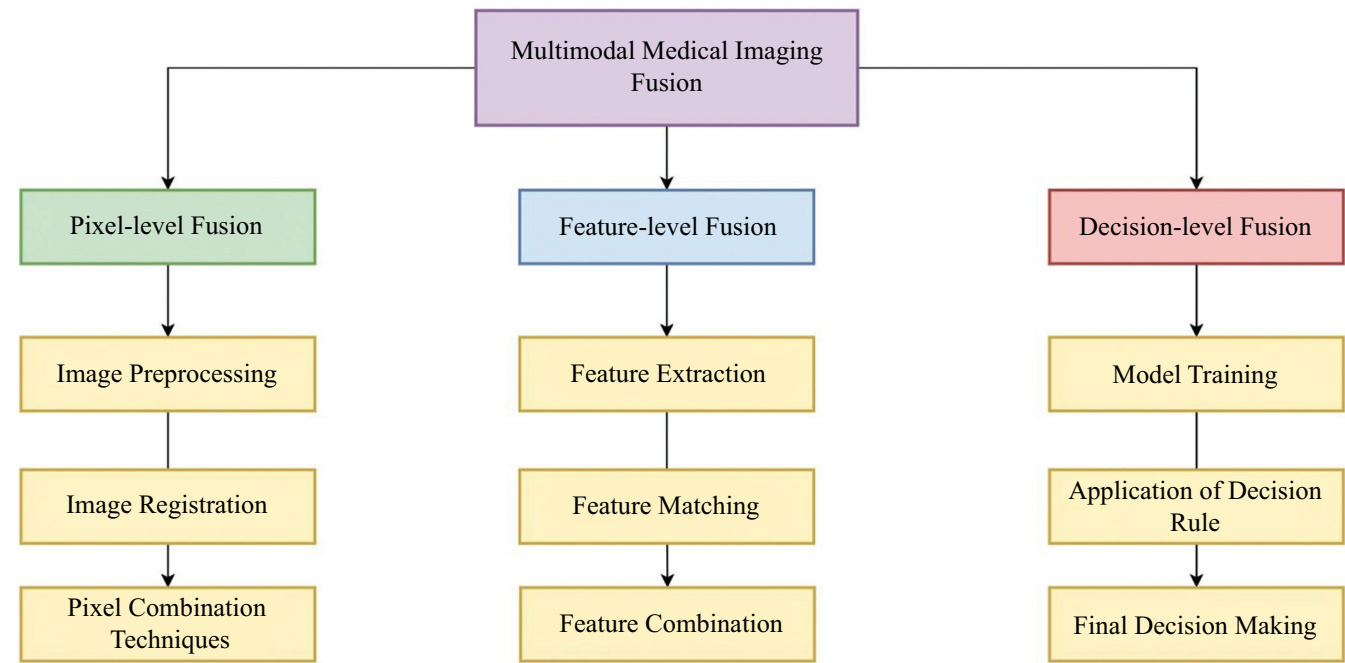


Fig. (7). Levels of multimodal medical image fusion.

Table 4. Fusion level vs. application scope.

Fusion Level	Description	Techniques	Advantages	Limitations	Typical Applications
Pixel-Level	Combines corresponding pixels from source images using arithmetic or transform-based methods	Averaging, Maximum Selection, DWT, NSCT, Shearlet	Preserves fine structural details; computationally simple	Highly sensitive to noise and registration errors	MRI-CT fusion in brain imaging; PET-CT for tumor mapping
Feature-Level	Extracts and fuses intermediate features such as edges, texture, and gradients before reconstruction	SIFT, CNN features, sparse representation, PCA	Robust to alignment errors; preserves semantic content	High computational complexity; depends on effective feature extraction	Alzheimer's analysis using MRI-PET; tumor segmentation from hybrid MRI
Decision-Level	Fusion occurs after independent modality analysis at the classification or prediction stage.	Majority voting, Bayesian inference, ensemble fusion	Allows modality-specific models; lower dependence on pixel accuracy	Does not generate a fused image; interpretability is reduced	CAD systems for tumor detection, AI-based diagnosis integration

Feature-level fusion can be categorized according to the nature of the methodologies used and the combined features. These techniques can be broadly categorized into sparse representation methods and clustering-based methods. Sparse techniques express images as sparse vectors in a dictionary. These methods typically divide source images into patches, organize them into vectors, and then perform the fusion process. Clustering algorithms, including Quantum Particle Swarm Optimization and Fuzzy C-means, can split feature spaces and provide weighting factors for fusion.

3.3.3. Decision-level Fusion

At the decision level, fusion occurs after separate processing and classification of input images. This is

commonly used in Computer-Aided Diagnosis (CAD) systems and is especially relevant in AI-based clinical workflows. Methods for decision-level fusion include majority voting, Bayesian inference, Dempster-Shafer theory, and ensemble learning techniques, which weigh individual decisions to derive a robust outcome. While decision-level fusion is less sensitive to registration errors and allows for modality-specific preprocessing and modeling, it lacks spatial resolution in the final output. It is generally unsuitable when a fused image is required for direct interpretation [17]. A brief comparison of these three, along with the scope of application, is summarized in Table 4.

3.4. Validation and Evaluation

Validation assesses the quality and clinical utility of the fused image using objective metrics and, where possible, expert evaluation. The most commonly used metrics include:

- Structural Similarity Index (SSIM): Measures perceived image quality and structural preservation.
- Peak Signal-to-Noise Ratio (PSNR): Evaluates image fidelity based on pixel intensity.
- Mutual Information (MI): Quantifies the amount of shared information between fused and source images.
- Entropy (EN): Reflects information richness in the fused image.
- Edge Preservation Index (EPI) and Spatial Frequency (SF): Measure edge clarity and texture detail [18].

Visual comparison remains essential in clinical validation. Radiologists or clinical experts often review Fusion outputs to assess diagnostic relevance and interpretability. Increasingly, evaluation also includes testing downstream tasks such as segmentation, classification, and localization to assess the practical benefits of fusion. MMIF is a multi-stage process where each phase requires tailored algorithms and quality checks to ensure robust performance, from preprocessing to validation. Fusion can be applied at different levels depending on the application, with each level offering unique advantages. Recent advances, especially in deep learning and transformer models, have improved registration accuracy and fusion robustness, allowing real-time, scalable implementations in clinical environments. The modular nature of the MMIF makes it adaptable, allowing hybrid strategies that combine pixel, feature, and decision-level fusion to maximize clinical

efficacy [19]. The various steps in the entire workflow are depicted in Fig. (8).

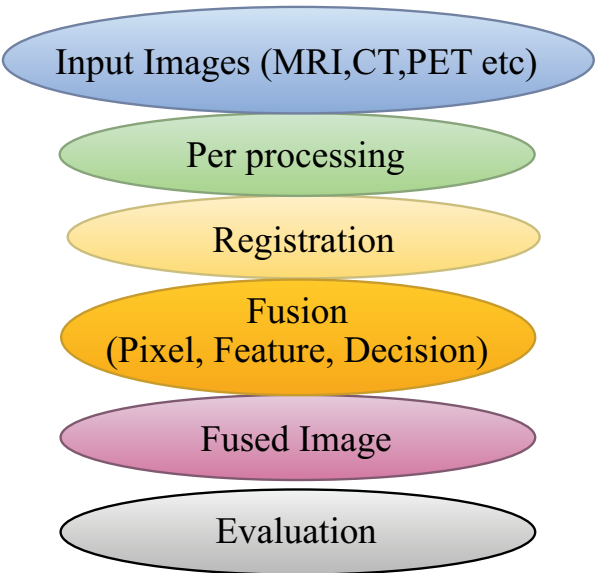


Fig. (8). MMIF workflow [19].

4. FUSION DOMAINS AND TECHNIQUES

These MMIF methods are used in diverse computational realms, which impart unique advantages. The choice of domain affects the efficiency, quality, and real-world applicability of fusion results. The prominent domains and their respective techniques are described in Fig. (9).

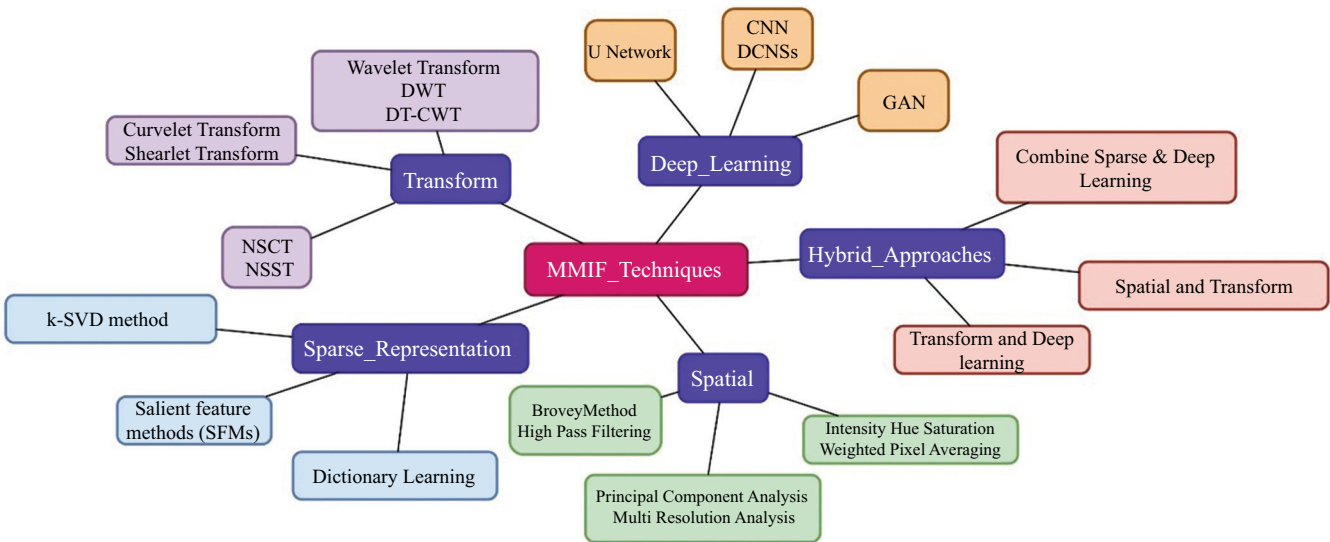


Fig. (9). Various domains of multimodal medical image fusion along with techniques.

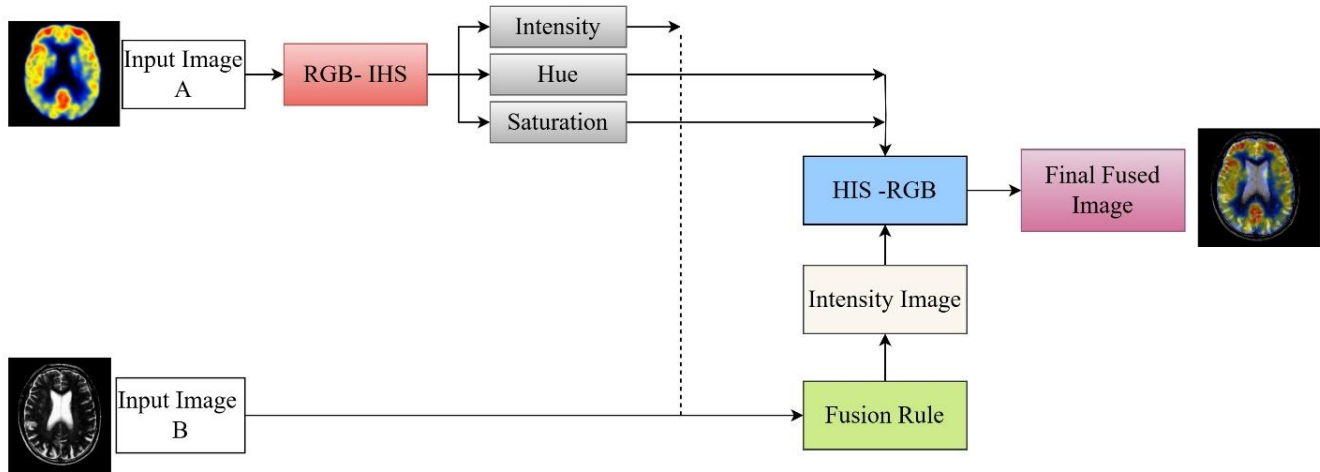


Fig. (10). Fusion of SPECT and MRI images using IHS in the spatial domain [19].

This section presents a structured review of the dominant fusion domains under five headings:

- Spatial Domain
- Frequency /Transform Domain
- Sparse representation
- Deep learning, and
- Hybrid Domain.

4.1. Spatial Domain

Image fusion in the spatial domain is distinguished by simple computation and sound handling, which can be easily used and processed. In this process, image fusion is performed using methods that manipulate pixel values without first transforming them into frequency domain formats. Conventional spatial fusion methods include Principal Component Analysis (PCA), Intensity-Hue-Saturation (IHS) mapping, Brovey transformation, and high-pass filtering. Such methods have the advantage of simplicity, faster execution times, and more vivid color expression, making them suitable for real-time cases and applications where computational power is limited. For instance, SPECT-MRI fusion has opportune over the IHS-based methods, which enhance the blending of anatomical and functional views without involving complex computational routines, as shown in Fig. (10).

Spatial domain methods tend to cause edge softening, spectral distortion, and weak noise tolerance. Since these techniques lack frequency composition, they cannot capture subtle textural and high-frequency details, and thus their role in complex applications such as brain tumor localization or microvascular imaging cannot be fully realized. Initial Studies by Baraiya and Gagnani [20] and Parekh *et al.* [21] highlighted traditional techniques like Principal Component Analysis (PCA) and Brovey Transform, which are utilized in fields such as remote sensing and preliminary diagnostic systems. These methods highlighted fundamental spatial integration while exposing significant

problems, including spatial distortions and inadequate spectral preservation. Morris and Rajesh [22] recognized the constraints of static fusion rules, advocating for image-adaptive approaches. Bhuvaneswari and Dhanasekaran [23] identified that conventional spatial domain techniques diminish image contrast, prompting the advancement of transform-domain solutions.

Li *et al.* [24] and Du *et al.* [25] made significant advancements by incorporating multi-scale transforms and edge-preserving filtering, thereby enhancing both structural integrity and contrast preservation. Their efforts established the foundation for hybrid spatial-transform techniques. Zhan *et al.* [26] tackled brain image fusion by implementing guided filtering and spatial gradient-based enhancements, which demonstrated enhanced performance in high-detail areas like cerebral tissue and lesions. Kotian *et al.* [27] conducted a comparative analysis, suggesting that a spatial/wavelet hybrid approach, which combined both spatial and spectral attributes, is a recommended method for general Multi-Image (MI) fusion. From 2018-2023, the field underwent substantial maturation when researchers such as Liu *et al.* [28], Na *et al.* [29], Saboori and Birjandtalab [30], and Pei *et al.* [31] employed wavelet transforms, multi-resolution decomposition, and guided filtering to preserve feature layers and minimize distortion. They attained significant success in applications including PET-MRI, CT-MRI fusion, and brain pathology analysis. Tan *et al.* [32], Chen *et al.* [33], and Deepali Sale [34] focused on enhancing low-complexity algorithms for rapid implementation in real-time systems, whereas Kong *et al.* [35], Li *et al.* [36], Feng *et al.* [37], and Zhang *et al.* [38] introduced sophisticated spatial techniques such as Framelet Transform, quasi-bilateral filtering, and structural dissimilarity metrics. These recent methodologies show enhanced performance in terms of structural retention, contrast preservation, and computational efficiency relative to State-of-the-Art (SOTA) fusion techniques. The progression of spatial domain techniques indicated a trend towards hybridization, multi-scale modeling, and adaptive

spatial decision-making, thereby enhancing robustness in clinical applications such as lesion localization, radiotherapy planning, and neuroimaging diagnostics. Table 5 depicts the fusion strategy and area of application in the spatial domain.

4.2. Transform Domain

The transform or frequency domain has emerged as a powerful approach to mitigate several challenges associated with secure image fusion. Leading up to these transformations is the conversion of images using conversion algorithms such as the Fourier Transform, Discrete Wavelet Transform (DWT), Non-Subsampled

Contourlet Transform (NSCT), or Laplacian Pyramid method. These changes separate images into separate spatial-frequency components, thus allowing for a more accurate separation of structural vs. textural aspects. Thereafter, when fusion is carried out in the transform domain, the reconstructed final image features an inverse transformation. Since frequency-based approaches excel at maintaining edge sharpness and texture information, they are suitable for clinical endeavors involving precise structure separation, such as identifying tumor edges. The basic process of decomposition and application of the inverse transform is shown in Fig. (11).

Table 5. Summary of spatial domain methods in medical image fusion.

Author (Year)	Technique	Method	Fusion Strategy	Area of Application
Baraiya & Gagnani (2014) [20]	PCA, direct pixel integration	Classical Spatial	Basic fusion using PCA for improved interpretability	Computer vision, medical imaging
Parekh et al. (2014) [21]	Brovey Transform, Color Model	Spatial	Color normalization and red channel enhancement; prone to spatial distortion	Remote sensing, radiology
Morris & Rajesh (2015) [22]	Pixel arithmetic (avg, add, subtract)	Spatial	Emphasized input-based method selection; basic fusion is not always optimal	Diagnostic imaging
Bhuvaneswari & Dhanasekaran (2016) [23]	Spatial vs. Transform	Comparative Study	Highlighted contrast loss in spatial fusion; promoted hybrid alternatives	MRI-CT, PET fusion
Li et al. (2017) [24]	Multi-scale + edge preserving filter	Spatial-Transform Hybrid	Proposed framework to preserve detail in structural fusion	Clinical diagnostics
Du et al. (2017) [25]	Local Laplacian filtering + multi-scale framework	Spatial	Used predefined features for distortion-free PET-SPECT fusion	Brain imaging
Zhan et al. (2017) [26]	Fast gradient filtering + morphological closure	Gradient-Based Spatial	Introduced fast structure-preserving filters; reduced execution time	Multi-organ fusion
Kotian et al. (2017) [27]	Comparative analysis	Spatial / Wavelet Hybrid	Recommended combination of spatial and spectral attributes	General MI fusion
Liu et al. (2018) [28]	Multi-scale joint decomposition + shearing filters	Transform Hybrid	Directional coefficients for high-detail retention	Brain functional imaging
Na et al. (2018) [29]	Filter-guided wavelet fusion	Wavelet/Spatial	Accurate localization of anatomical targets	CT-MRI fusion
Saboori & Birjandtalab [30]	Adaptive filtering + spectral-spatial optimization	Spatial	Structural and spectral enhancement through filter parameter tuning	Biomedical instrumentation
Pei et al. (2020) [31]	Guided filtering + multiscale layers	Spatial + Texture Layering	Preserved structural layers and enhanced image contrast	Multi-organ medical imaging
Tan et al. (2021) [32]	Three-layer image fusion	Spatial Layering	Validated on >100 image pairs from multiple pathologies	Collaborative diagnosis
Chen et al. (2021) [33]	Rolling Guidance Filtering	Spatial	Separated and fused structural-detail layers; maintained anatomical clarity	Head and brain imaging
Deepali Sale (2022) [34]	PCA, ICA, Averaging	Classical Spatial	Advocated low-complexity spatial fusion for fast implementation	Low-resource medical devices
Kong et al. (2022) [35]	Framelet Transform + Subband fusion	Framelet / Spatial	Improved structure clarity via GDGFRW and SWF modules	Radiology, Lesion detection
Li et al. (2023) [36]	Modified Laplacian + Local Energy	Spatial Energy-based	Enhanced feature energy preservation; outperformed 9 SOTA methods	Harvard dataset
Feng et al. (2023) [37]	SSD for detail and texture retention	Structural Similarity	Solved low contrast and pseudo-edges using structure-preserving fusion	Clinical diagnosis (multi-pathologies)
Zhang et al. (2023) [38]	Quasi-cross bilateral filtering (QBF)	Spatial Filtering	Focused on edge contour, lesion detail, and contrast; high benchmark performance.	PET/MRI fusion, Neurology

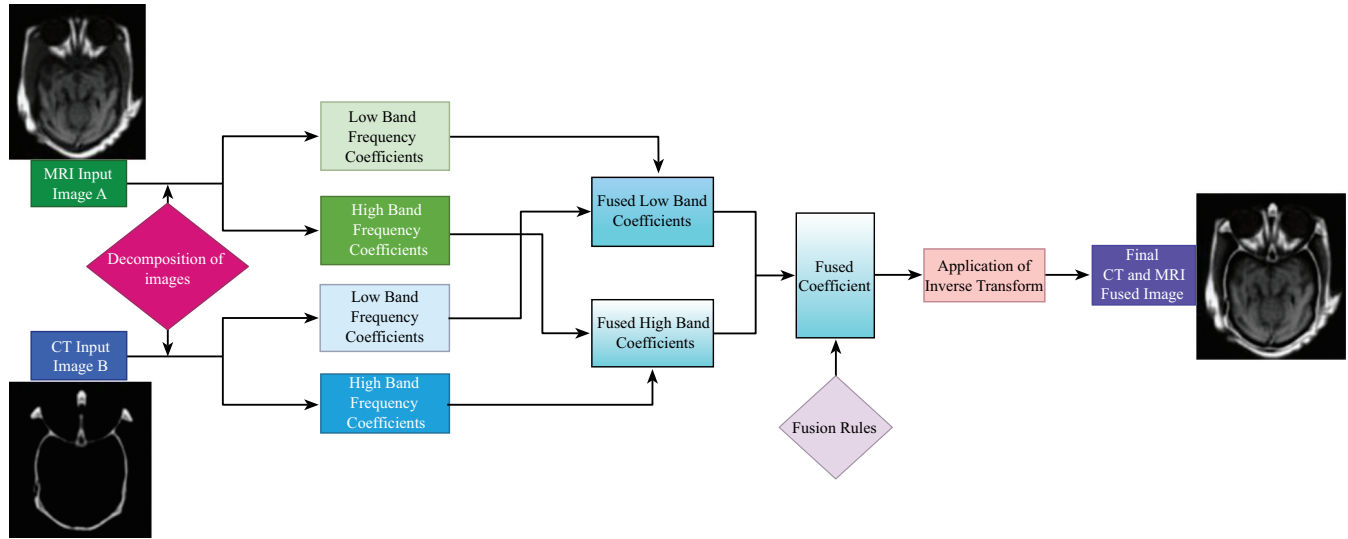


Fig. (11). Basic methodology of CT and MRI fusion in the transform domain described along with CT and MRI images from AANLIB [19].

Preliminary research, including that of Singh and Khare [39], tackled the shortcomings of real-valued wavelet transforms, specifically shift sensitivity and inadequate directionality by utilizing the Dual-Tree Complex Wavelet Transform (DCxWT). This method markedly enhanced fusion results by maintaining phase and directional specifics. In the same year, Ganasala and Prasad [40] introduced an image fusion technique for CT and MR images with the Nonsubsampled Contourlet Transform (NSCT), resulting in improved visualization of soft tissue and osseous structures. Bhateja *et al.* [41] advanced this research by developing a two-stage architecture that included Stationary Wavelet Transform (SWT) and NSCT, utilizing PCA for redundancy minimization and contrast enhancement.

To more effectively capture edge information, Srivastava *et al.* [42] utilized the Curvelet Transform, which showed enhanced efficacy in maintaining anisotropic features and improving visual perception via a local energy-based fusion rule. Xu *et al.* [43] presented the Discrete Fractional Wavelet Transform (DFRWT), which, due to its fractional order parameters, facilitated adaptive decomposition and enhanced multimodal image fusion efficacy. Gomathi and Kalaavathi [44] demonstrated that the NSCT method provides improved frequency decomposition while efficiently preserving high-frequency image components. In contrast, Liu *et al.* [45] showed that the NSST is highly effective in maintaining texture and detail. Numerous scholars investigated shearlet-based and nonsubsampled techniques for improved frequency decomposition. Gambhir and Manchanda [46] also demonstrated that the fused images obtained from the proposed method offer better clarity and enhanced

information, making them more useful for quick diagnosis and improved treatment of diseases.

Li *et al.* [47] improved fusion efficacy by utilizing NSST with a novel fusion rule that reduced blocking and blurring artifacts through local coefficient energy and mean-based methodologies, while Ganasala and Prasad [48] implemented SWT with Transformation Error Minimization (TEM) to improve image fusion quality while decreasing computational load. Goyal *et al.* [49], Khare *et al.* [50], and Kong *et al.* [51] enhanced image fusion by preservation of edges, textures, and structural boundaries, minimizing artifacts with RGF/DTF, median-based NSST, and Framelet Transform, respectively. The results of the work by Diwakar *et al.* [52] demonstrated that non-conventional transform domains yield improved outcomes when integrated with various spatial domain architectures. An overview of various transform techniques is presented in Fig. (12). Although distinguished by their quality enhancements, frequency domain approaches are accompanied by increased computational costs and high requirements for exact image registration, which may be quite challenging to implement in practice. The key contributions are presented in Table 6.

4.3. Sparse Representation

The sparse representation-based fusion method provides a more compacted, higher information-to-data ratio. Sparse methods examine images by projecting them onto a dictionary of basis functions, which can be trained or predetermined. The focus is on a small set of coefficients that correspond to significant aspects of the image. By combining coefficients from different modalities, as shown in Fig. (13), the method constructs a fused image with enhanced predominant structure and contrast.

Table 6. Key contributions from the transform domain.

Study	Methodology	Key Contributions
Singh and Khare [39]	Dual-Tree Complex Wavelet Transform (DCxWT)	Addressed the constraints of wavelet transforms, such as shift sensitivity, poor directionality, for better fusion.
Ganasala and Prasad [40]	Nonsubsampled Contourlet Transform (NSCT)	Improved visualization of soft tissue and bone structure, enhancing the quality of image fusion.
Bhateja et al. [41]	SWT + NSCT with PCA	Developed a dual-stage architecture for contrast enhancement and redundancy minimization.
Srivastava et al. [42]	Curvelet Transform	Effectively captured anisotropic features and improved visual perception with a local energy-based fusion rule.
Xu et al. [43]	Discrete Fractional Wavelet Transform (DFRWT)	Delivered adaptive decomposition for enhancing fusion performance across modalities.
Gomathi and Kalaavathi [44]	NSCT	Improved frequency decomposition efficiently maintains high-frequency image components.
Liu et al. [45]	Nonsubsampled Shearlet Transform (NSST)	Successfully maintain texture and detail effectively.
Li et al. [47]	NSST with novel fusion rule	Addressed blocking and blurring artifacts using local coefficient energy and a mean-based fusion technique.
Ganasala and Kumar [48]	SWT with Transformation Error Minimization (TEM)	Optimized performance with less computational load and improved image fusion quality.
Goyal et al. [49]	Rolling Guidance Filtering (RGF) and Domain Transfer Filtering (DTF)	Maintained edge and texture details while fusing low-resolution images.
Khare et al. [50]	Median-based fusion rule within NSST	Preserved structural boundaries through median-based fusion.
Kong et al. [51]	Framelet Transform (FT)	Resolved fusion artifacts and texture degradation by decomposing images into structured layers.

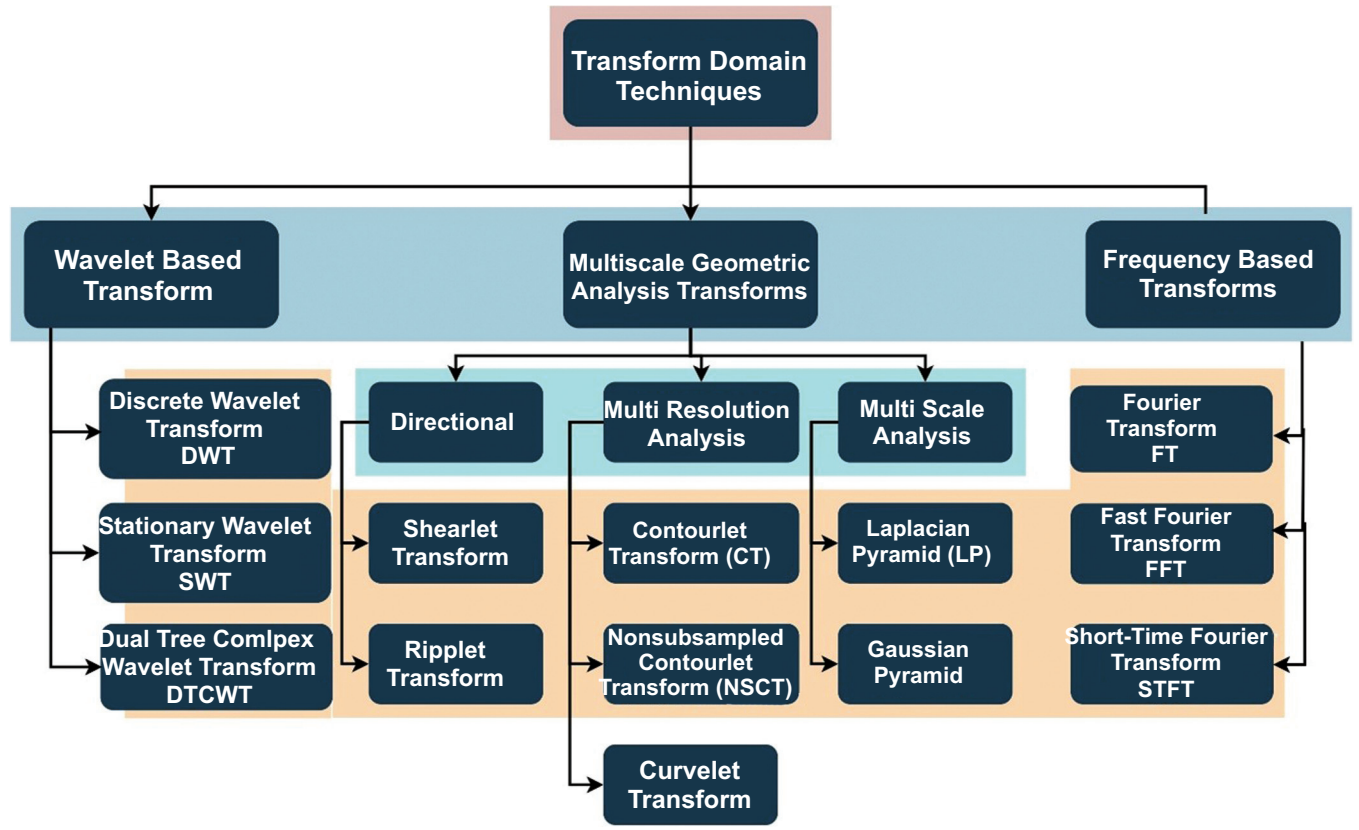


Fig. (12). Overview of different techniques of the transform domain.

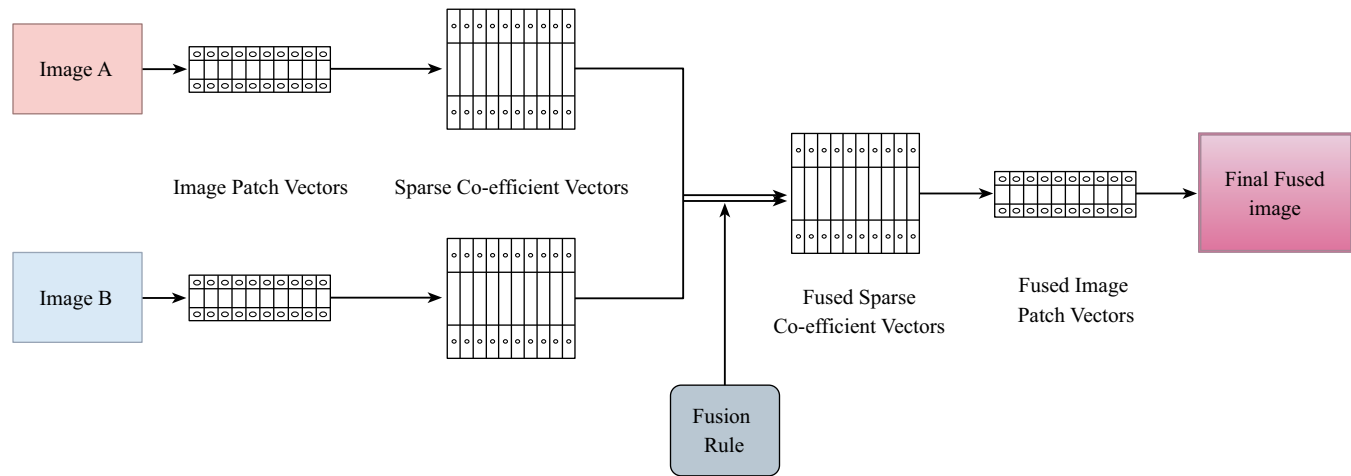


Fig. (13). Steps of image fusion using sparse representation methods [53].

It has gained significant interest because of its ability to maintain prominent image elements such as edges and textures while minimizing redundancy. A typical SR-based image fusion process comprises the following steps:

1. Extraction of patches from source images (such as CT and MRI).
2. Encoding of each patch with a trained dictionary.
3. Integration of sparse coefficients by a criterion (*e.g.*, max-selection or averaging).
4. Reconstruction of amalgamated patches to achieve the final image [53].

Zhang *et al.* [54] described how the SR model forms a dictionary through a sparse linear combination of prototype signal models. According to Joint Sparse Representation (JSR), several signals from several sensors of the same scene constitute an ensemble. While each signal possesses an innovative sparse component, they all share a common sparse component. As compared to SR, the JSR presents reduced complexity. Zong and Qiu [55] proposed a sparse method using categorized image patches based on their geometric orientation. Liu *et al.* [56] made a significant early contribution by introducing

Convolutional Sparse Representation (CSR), an alternate representation of SR using the convolutional form, aiming to achieve SR of a complete image rather than a localized image patch.

Liu *et al.* [57] presented Convolutional Sparsity-based Morphological Component Analysis (CS-MCA). In contrast to the conventional SR model, which relies on a single image component and overlapping patches, the CS-MCA model can concurrently accomplish multicomponent and SRs of the source images by amalgamating MCA and CSR within a cohesive optimization framework. Shabanzade and Ghassemian [58] employed sparse representation in the NSCT (Nonsubsampled Contourlet Transform) domain in a hybrid context. Their approach integrated low-frequency coefficients through sparse coding and high-frequency components using max-selection, resulting in both multiscale decomposition and sparse adaptability. Alternative hybrid methodologies have integrated SR with PCNN (Pulse Coupled Neural Networks), and clustering-based multi-dictionary learning, which allocates region-specific dictionaries (*e.g.*, for edges *versus* smooth regions) to enhance localization and context-aware fusion. The various categories of sparse methods are also described in Table 7.

Table 7. Categories of sparse representation methods.

Category	Model
Local and single-component SR-based	Orthogonal Matching Pursuit (OMP), Simultaneous OMP (SOMP), Group Sparse Representation (GSR), Sub-dictionary-based adaptive SR combined with other transforms
Multi-component SR-based	Joint Sparse Representation (JSR), Morphological Component Analysis (MCA)
Global SR-based	Convolutional Sparse Representation (CSR)
Simultaneous multi-component and Global SR-based	MCA-extended version of CSR

Table 8. Challenges of sparse representation methods in image fusion.

Aspect	Challenges
Feature Preservation [53]	Poor dictionary training can result in suboptimal fusion outcomes.
Adaptability [53]	The process of dictionary learning is computationally intensive and requires substantial training data, posing challenges in resource-constrained environments.
Robustness to Misregistration [60]	Significant misregistration can still degrade fusion performance, necessitating precise alignment in practice.
Computational Complexity [61]	SR methods are computationally demanding, which limits their applicability in scenarios requiring rapid processing.
Noise Sensitivity [62]	SR methods may inadvertently amplify noise, compromising image quality if the noise characteristics are not well understood.

SR continues to serve as a robust intermediary solution between conventional and deep learning-based fusion approaches. Its unsupervised characteristics and adaptability render it especially advantageous in contexts with limited labeled data. As highlighted in the paper by Hermessi *et al.* [59], SR remains fundamental to numerous advanced approaches, particularly in hybrid fusion architectures where it enhances contrast, clarity, and feature retention [60]. When sparse representation is utilized alongside multi-scale techniques, such as NSCT, Laplacian Pyramid, Dual Tree Complex Wavelet, or Curvelet, it effectively improves fine details, boosts contrast, and minimizes noise. According to a review by Zhang *et al.* [61], sparse representation proved superior to traditional multi-scale approaches in terms of retaining image structures and defining edges. It learns an overcomplete dictionary from a set of training images, resulting in more stable and significant results. A smart blending approach that combines SR with SCNN to overcome flaws such as edge blurriness, diminished visibility, and blocking artifacts was proposed by Yousif *et al.* [62]. The results have demonstrated that the proposed method is superior to previous techniques, particularly in suppressing the artifacts produced by traditional SR and SCNN methods. Table 8 summarizes the advantages and challenges of this domain. SR-based approaches encounter constraints, including:

- The high computational cost results from sparse optimization procedures.
- Block artifacts arising from independent patch-based judgements.
- Sensitivity to misregistration, as the majority of approaches presume aligned inputs.

4.4. Deep Learning Fusion Methods

The last few years have seen a paradigm shift in MMIF research, with deep learning shaping into an enabler of automated multimodal fusion through end-to-end learning architectures. Although Deep Neural Networks (DNNs) have yielded exceptional results in learning multi-level feature representations from raw image data, the architects of the networks are finding it difficult to give them meaningful names. Notable compositions of DNNs have been CNNs, U-Nets, and Generative Adversarial Networks (GANs). The training objective of these models incorporates optimal structural alignment, maintaining semantic information, and enhancing disease identification.

The initial implementation of CNNs in medical image fusion was presented by Liu *et al.* [56], exhibiting superior performance as compared to spatial and transform domain approaches. CNNs' design effectively extracts spatial and textural information, yet they necessitate extensive annotated datasets and intricate tuning processes. Liu *et al.* [63] emphasized the dual roles of fusion rules and activity level estimation, using local filters and clarity maps to guide the amalgamation of high-frequency features. Gibson *et al.* [64] insisted upon the importance of deep networks for neurological diagnosis through pixel-level fusion.

Xia *et al.* [65] accomplished a significant advancement by integrating multiscale decomposition with CNNs, facilitating high/low-frequency discrimination and enhanced multi-resolution fusion. Wang *et al.* [66] employed Siamese CNNs to create activity-guided weight maps, resulting in structurally intricate fused images. To overcome batch processing restrictions, Li *et al.* [67] created CNN-based frameworks that facilitated real-time, multimodal fusion, therefore improving efficiency and detail retention. These approaches provided practical utility in clinical environments requiring simultaneous processing of many images. The fusion approach using CNN and autoencoders is depicted in Fig. (14).

Chuang *et al.* [68] introduced a fusion framework that integrated U-Net and Autoencoder architectures (FW-Net), where the encoder-decoder configurations exhibited U-Net's skip connections. The design, initially limited to CT-MRI, has the potential for future PET-MRI and SPECT fusion. Kumar *et al.* [69] examined the utilization of CNNs for thermal-visual fusion in remote sensing, showing cross-domain relevance. El-Shafai *et al.* [70] introduced a hybrid fusion technique in which CNNs integrated three images using traditional methods, leading to less redundancy and enhanced semantics.

To address the issues of semantic degradation in fused outputs, Ghosh [71] introduced a dual U-Net FW-Network that prioritized semantic-level fusion. This approach markedly enhanced clinical utility in disease localization and segmentation. Deep learning-based image fusion is a powerful paradigm that provides excellent visual fidelity, task adaptability, and end-to-end automation. However, accessible data sets, interpretable models, and the creation of computationally efficient architectures that work across modalities are necessary for the advancement.

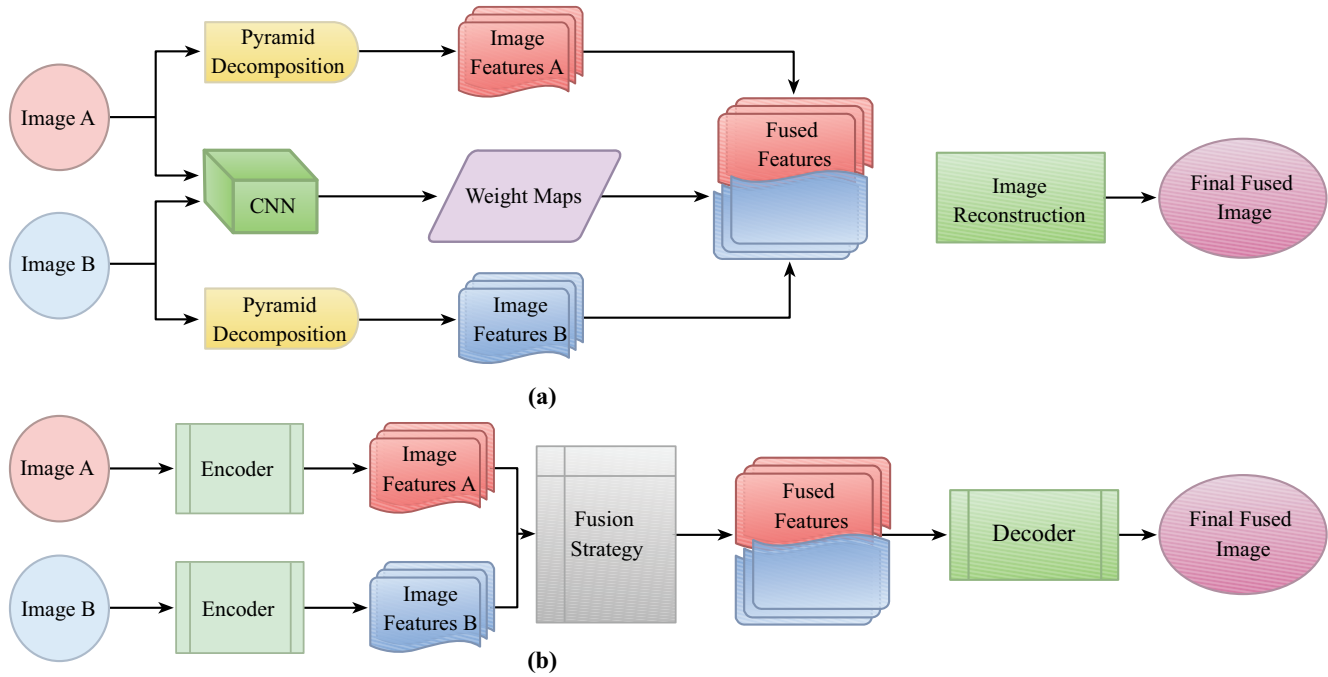


Fig. (14). Different approaches of deep learning (a) CNN-based fusion (b) Autoencoder-based fusion [2].

A CNN-based multimodal fusion approach designed for oncology not only succeeded in improving diagnostic accuracy but also outperformed current methods in both subjective and objective metrics. Due to their generative properties, GANs can create high-resolution fused images that preserve both anatomical structure and functional intensity. The dependence of such models on large sets of labeled data and their tendency to overfit limited data variability are serious issues. The lack of interpretability is also a concern for these models in clinical settings. Figure 15 demonstrates the domain-wise publication trends across Web of Science, in multimodal image fusion from 2000 to 2024. It indicates the rapid proliferation of deep learning and hybrid domains in this period. Driven by the endorsement of CNNs, U-Nets, and GANs, the adoption of deep learning methodologies has shown remarkable expansion. The explosion in growth indicates a shift in the sphere towards using data-driven fusion techniques, characterized by a strong understanding and fusion of intricate anatomical and functional relationships.

At the same time, the development of hybrid approaches using such spatial, frequency, and deep learning approaches is relatively stable, demonstrating their ability to handle the dissimilar nature of medical data. Due to their modular structure, these techniques provide superior flexibility and precision, which improves overall fusion performance. Collectively formed by these advances, these fields have outperformed traditional approaches and indicate a shift towards smarter, more holistic fusion methods for medical applications. MMIF's future research appears to be majorly focused on DL-based and hybrid techniques, especially where complex cases of oncology and

neuroimaging are involved. The key contributions from DL are presented in Table 9.

4.5. Hybrid Domain

To benefit from diverse domains and tend towards their minimal negative effects, hybrid fusion approaches have attracted much attention. Such approaches utilize specific domain expertise, such as NSCT for frequency analysis and CNNs for feature extraction, or the use of neural networks. Simultaneously managing the spatial, frequency, and contextual information, hybrid systems are capable of creating informative fused images.

Xia *et al.* [72] established a foundational framework by combining Nonsubsampled Contourlet Transform (NSCT) and Dual-Tree Complex Wavelet Transform (DTCWT), which was supplemented by Pulse-Coupled Neural Networks (PCNN) for the creation of composite images. This represented a crucial advancement in integrating hand-crafted and adaptive transformations to tackle challenges such as image noise and resolution discrepancies. Wang *et al.* [73] improved diagnostic precision by employing NSST and adaptive decomposition frameworks that consider high/low frequency layers and dynamic textural features, respectively. These works acknowledged that conventional static decomposition inadequately reflects contextual differences across modalities. Bhateja *et al.* [74] advanced the hybrid approach by introducing shearlet and NSCT-based fusion for PET/SPECT, MRI, and CT images, including contrast enhancement and weighted PCA to preserve multispectral integrity. Du *et al.* [75] and Zhao *et al.* [76] tackled modality-specific inconsistencies by developing distinct methodologies for MRI and PET, thereby enhancing fusion accuracy through edge-based weighting.

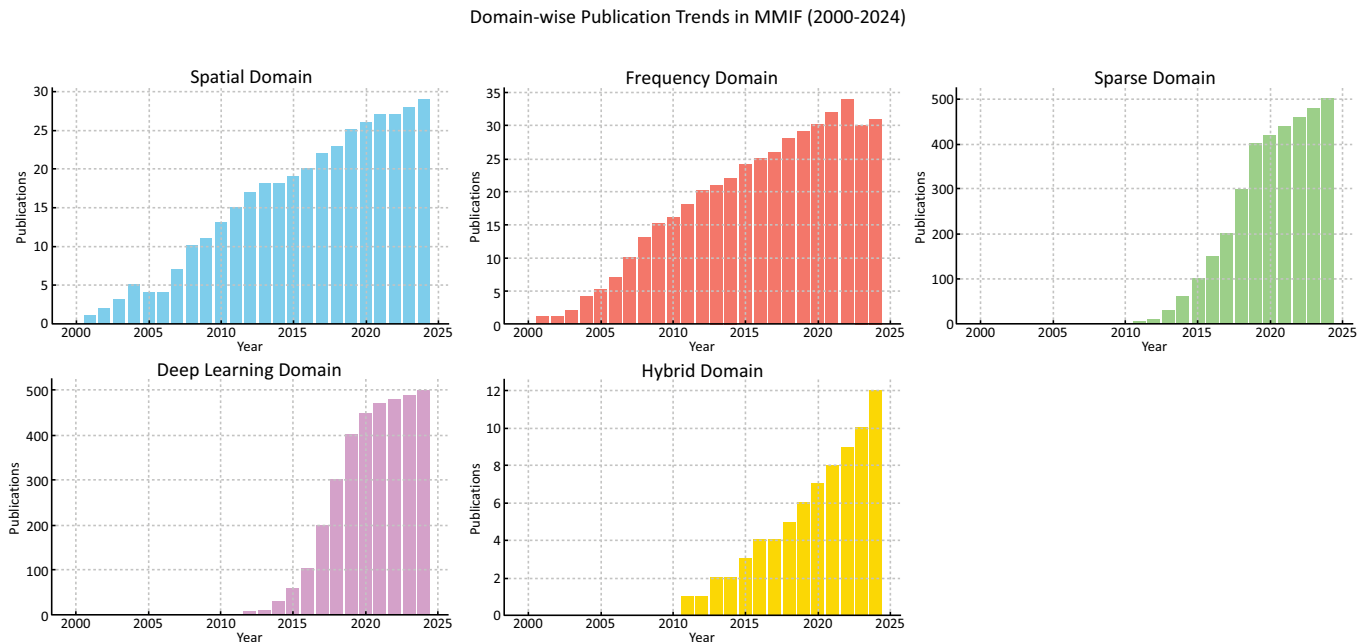


Fig. (15). Publication trends across all domains over the last five years (WOS).

Table 9. Key contributions from deep learning.

Study	Methodology	Key Contributions
Liu <i>et al.</i> [56]	Convolutional Neural Networks (CNNs)	Exhibited better performance as compared to spatial and transform domain methods, highlighting the capability of CNN to extract spatial and textural characteristics.
Liu <i>et al.</i> [63]	CNNs with fusion rules and activity level estimation	Implemented local filters and clarity maps to facilitate the integration of high-frequency features, enhancing fusion quality.
Gibson <i>et al.</i> [64]	Deep networks	Highlighted the significance of deep learning in neurological diagnosis and enhancing fusion at the pixel level for diagnostic accuracy.
Xia <i>et al.</i> [65]	Multiscale decomposition combined with CNNs	Better division of high/low-frequency components, facilitating detailed and multi-resolution fusion.
Wang <i>et al.</i> [66]	Siamese CNNs with activity-guided weight maps	Increased structural richness in final fused images <i>via</i> activity-guided weight maps. Enhancing the retention of essential features
Li <i>et al.</i> [67]	CNN-based	Concentrated on real-time processing of multimodal images, providing practical utility in clinical settings.
Chuang <i>et al.</i> [68]	Fusion U-Net and Autoencoder (FW-Net)	A hybrid encoder-decoder structure was introduced, with potential for further expansion to PET-MRI and SPECT fusion.
Kumar <i>et al.</i> [69]	CNNs	Proposed cross-domain applications, using CNNs for thermal-visual fusion.
El-Shafai <i>et al.</i> [70]	Hybrid CNN-based fusion pipeline	Combined three images using traditional approaches, providing a reduction in redundancy and enhancing the semantic quality in fused outputs.
Ghosh [71]	Dual U-Net FW-Network	Concentrated on enhancing disease localization and segmentation by addressing semantic degradation in fused outputs.

Maqsood and Javed [77] employed two-scale decomposition with spatial gradients to enhance edges. Wang *et al.* [78] and Liu *et al.* [79] employed adaptive sparse coding and total variation transformations, enhancing detail retention while diminishing high-frequency noise. Yadav [80] utilized independent and principal component

analysis using a wavelet framework but observed residual noise and artifacts. In their study, Ashwanth and Swamy [81] showed that the Stationary Wavelet Transform (SWT) surpasses the standard Discrete Wavelet Transform (DWT) in terms of entropy preservation. Huang *et al.* [82] emphasized that while hybrid models enhance established

frameworks, problems persist, especially in feature extraction and color distortion. These constraints stimulated investigation into hybrid deep learning strategies. Kaur *et al.* [83] integrated ANFIS with cross-bilateral filtering, resulting in enhanced entropy (2.92), and suggested volumetric fusion for future neuroimaging applications. Kaur *et al.* [84] conducted a systematic review emphasizing the necessity for precise, reliable, and interpretable fusion techniques.

Polinati *et al.* [85] and Li *et al.* in 2021 [86] introduced innovative frameworks employing Variational Mode Decomposition (VMD), local energy gradients, and bilateral filtering, all designed to improve clarity and reduce luminance deterioration. Zhu *et al.* [87] and Alseelawi and Hazim [88] concentrated on enhancing NSST-DTCWT-based fusion techniques to achieve equilibrium between texture and structural integrity. Alseelawi's work prominently highlighted velocity and visual excellence, using PCNN as a guiding framework. Kalamkar and Geetha [89] utilized transfer learning with DWT, attaining enhanced structural similarity index values. Goyal *et al.* [90] developed a cross-bilateral, edge-preserving fusion filter that reduces artifacts while improving image quality. Likewise, Faragallah *et al.* [91] amalgamated CNN with three traditionally fused image sets to improve overall image quality and diagnostic efficacy. Zhou *et al.* [92] tackled issues of brightness degradation and detail retrieval by the application of NSST and Improved Structure Tensor (IST) decomposition, resulting in enhanced contrast while differentiating smoothing, edge, and corner layers.

Kittusamy and Kumar *et al.* [93] utilized Joint Sparse Representation (JSR) and NSCT to attain enhanced high perceptual clarity in MRI-CT fusion. Dinh [94, 95] formulated two complementary models to address inadequate contrast and edge degradation through a three-scale decomposition and local energy-based fusion rules. Balakrishna *et al.* [96] evaluated nine DWT-based combinations, validating the method's efficacy in the detection of abnormalities and clinical planning. Moghtaderi *et al.* [97] suggested a Multilevel Guided Edge-Preserving Filtering (MLGEPF) technique that combined computational expense with structural accuracy. Zhao *et al.* [98] proposed a novel method based on three-scale frequency decomposition along with SSIM-optimized feature blending, which significantly facilitates the process of fusing MRI and PET images for brain tumor examination. Various hybrid combinations, along with their advantages and disadvantages, are described in Table 10.

Table 11 signifies the evolving emphasis of research within Multimodal Medical Image Fusion (MMIF) over three distinct phases. Spatial domain methods prevailed in the initial period but have since been replaced by more sophisticated techniques. Frequency domain techniques have shown significant output growth and have sustained stability. Sparse representation techniques have transitioned from minimal utilization in their first stages to considerable significance in recent years.

Table 10. Various hybrid combinations along with advantages and disadvantages.

Author/ Year	Hybrid Combination	Advantages	Disadvantages
Xia <i>et al.</i> , 2018 [72]	NSCT + PCNN	Improves contrast; effective for multi-resolution fusion	Complex; sensitive to noise levels and parameter tuning
Wang <i>et al.</i> , 2018 [73]	Adaptive Decomposition + Texture Integration	Dynamic layer integration improves color and texture representation	Requires rule tuning; may introduce artifacts
Bhateja <i>et al.</i> , 2018 [74]	Shearlet + NSCT + Weighted PCA	High spectral-spatial fidelity; suited for PET/CT/MRI	Computationally intensive; color normalization required
Du <i>et al.</i> , 2019 [75]	Separate Decomposition for MRI and PET	Customized decomposition maintains modality-specific features	High design complexity; lacks real-time scalability
Wang <i>et al.</i> , 2020 [78]	Adaptive Sparse + Laplacian Pyramid	Minimizes noise in high-frequency ranges; adaptive sparsity	May be unstable with varying image types
Yadav and Yadav, 2020 [80]	Wavelet + ICA/PCA	Elementary; broadly applicable; improves interpretability	Noise sensitivity; potential overfitting
Ashwanth and Swamy, 2020 [81]	SWT vs DWT	SWT retains greater energy and detail compared to DWT	Requires precise coefficient tuning
Kaur <i>et al.</i> , 2021 [83]	ANFIS + Cross-Bilateral Filter	Enhanced entropy; edge detail maintained	Requires ANFIS model training and tuning
Faragallah <i>et al.</i> , 2022 [91]	CNN + Multi-Input Fusion	Efficient and effective; reduces redundancy	Quality depends on pretrained models
Kalamkar and Geetha, 2022 [89]	Transfer Learning + DWT	Improved structural similarity and generalization	Training requires large datasets
Zhou <i>et al.</i> , 2022 [92]	NSST + IST (Improved Structure Tensor)	Maintains brightness and local structure	Complex to implement; computationally heavy.
Kittusamy and Kumar, 2023 [93]	JSR + NSCT	Elevated contrast and detail retention in soft tissues	Requires dictionary learning; time-consuming
Dinh, 2023 [94]	Three-Scale Decomposition + Local Energy	Prevents information loss in edges; enhances contrast	Parameter tuning is crucial; risk of blur
Moghtaderi <i>et al.</i> , 2024 [97]	Guided Edge-Preserving Filtering (MLGEPF)	Prompt and reliable; balances performance and quality	Filter design and scale sensitivity
Zhao <i>et al.</i> , 2024 [98]	Guided Fusion (Smoothing + Global Optimization)	Maintains texture, noise, and structure clearly	May overlook fine details if the structure is misclassified

Table 11. Web of Science records illustrate the evolution of domain usage in MMIF.

Domain	Early Phase (2000-2010)	Growth Phase (2011-2017)	Boom Phase (2018-2024)
Spatial	High	Medium	Declining
Frequency	Medium	High	Stable
Sparse Representation	Very Low	Medium	High
Deep Learning	None	Emerging (post-2016)	Dominant
Hybrid	Low	Emerging	Rising sharply

Table 12. Comparative analysis of MMIF domains - advantages, limitations, and applications.

Domain	Advantages	Limitations	Typical Applications
Spatial Domain [19]	Elementary execution, Better color representation. Rapid computation	Edge blurring, Low SNR, Spectral distortion	SPECT-MRI fusion using HSV- X-ray/CT overlays
Frequency Domain [50]	Elevated SSIM- Good texture and edge preservation	Complex registration, High computational cost	Tumor localization (MRI-PET)- Brain mapping using NSCT and Laplacian Pyramid
Sparse Representation [60, 61]	Enhanced contrast clarity-Concise representation, Good noise removal	Artifacts from basis mismatch, Edge degradation	CT-MRI brain fusion utilizing K-SVD- Dictionary learning for tumor detection
Deep Learning [4, 64]	Automatically acquires complex features, High fusion accuracy	Requires large datasets, Risk of overfitting	U-Net fusion in COVID detection- GANs for whole-body PET/CT integration
Hybrid Domain [83, 88]	Combines domain strengths, High robustness	Increased model complexity, Difficult tuning	NSCT + PCNN fusion- DWT-IFS-PCA in multimodal cancer detection

Deep learning was nearly non-existent before 2016, but has become the dominant methodology. Hybrid approaches, which amalgamate multiple techniques, have experienced significant expansion, signifying a trend towards integrative and adaptive fusion approaches. A comprehensive analysis of Multimodal Medical Image Fusion (MMIF) domains emphasizing their strengths, weaknesses, and principal application areas is highlighted in Table 12.

5. APPLICATIONS OF IMAGE FUSION IN CLINICAL MEDICINE

This section highlights the integration of structural medical imaging modalities through fusion techniques and their clinical applications, especially in surgical planning, oncology, orthopedics, and neurosurgery. The following examples highlight recent advances and use cases where image fusion has improved diagnosis, treatment accuracy, and procedural efficiency.

5.1. Surgical Planning Using Synthetic CT from MRI

A recent study has explored the feasibility of generating synthetic Computed Tomography (CT) images of the lumbar spine from Magnetic Resonance Imaging (MRI) using a patch-based convolutional neural network. This approach aimed to support pre-operative planning without exposing patients to ionizing radiation using deep learning. The study involved three cases and demonstrated that deep learning-enabled MRI-to-CT conversion offers high-quality structural visualization, reducing radiation exposure compared to conventional CT scans (typically 3.5-19.5 mSv for spine imaging) [99].

5.2. Orthopedic Implant Design and Additive Manufacturing

The combination of CT and MRI has also been pivotal in the design of patient-specific orthopedic implants. These modalities are employed to capture comprehensive anatomical data, including size, shape, texture, and bone density. This facilitates the development of custom implants and allows for the reconstruction of traumatic bone defects through additive manufacturing technologies [100].

5.3. Management of Complex Fractures Using Rapid Prototyping

Fusion imaging has enabled advances in Rapid Prototyping (RP) and 3D reconstruction, particularly for complex fractures in anatomical regions such as the joints, acetabulum, and spine. RP assists surgeons in visualizing fracture geometry preoperatively, which improves the accuracy of anatomical reduction and reduces surgical time, anesthesia duration, and intraoperative blood loss [101].

5.4. Surgical Effects of Resecting Skull Base Tumors Using Preoperative Multimodal Image Fusion

A retrospective study was conducted on 47 patients with skull base tumors. Preoperative CT and MRI data acquisition were performed using GE AW workstation software for co-registration, fusion, and three-dimensional reconstruction of the brain. The surgical plan was designed based on multimodal images. The application of the fusion technique provided essential visual guidance in skull base tumor surgery, assisting neurosurgeons in accurately planning the surgical incision and precisely resecting the lesion [102].

5.5. Trigeminal Neuralgia Treatment with Integrated Neuro-Navigation

In 13 patients undergoing percutaneous radiofrequency trigeminal rhizotomy, the fusion of MRI and intraoperative CT (iCT) images provided improved anatomical delineation of the trigeminal cistern. This integration supports more accurate targeting, especially in recurrent cases of trigeminal neuralgia. The study emphasized the benefits of fusion-guided neuro-navigation and suggested that longer follow-ups are needed to assess long-term therapeutic efficacy [103].

5.6. Frameless Stereotactic Radiosurgery with Gamma Knife Icon

In a clinical series of 100 patients, MRI-CBCT (Cone Beam CT) fusion was utilized for frameless stereotactic radiosurgery using the Gamma Knife Icon. MRI provided superior soft tissue contrast, while CBCT served as the baseline for stereotactic registration. The adaptive dose distribution was computed based on the patient's real-time geometry after fusion, optimizing treatment accuracy. This method overcomes the limitations of traditional CT-guided radiotherapy by ensuring better alignment of tumor and anatomical landmarks [104, 105].

5.7. Image Fusion in Precision Medicine for Oncology

In the context of precision oncology, fusion imaging technologies are increasingly used to enhance diagnostic accuracy and individualized treatment planning. The integration of CT, MRI, and PET enables better visualization of tumor morphology and metabolic activity, facilitating more accurate localization and classification of malignancies. Such multimodal fusion approaches are pivotal in improving therapeutic outcomes and reducing harm to healthy tissue [106].

5.8. Image Fusion in the Diagnosis and Treatment of Liver Cancer

The rapid advancement of medical imaging has facilitated the effective application of image fusion technology in diagnosis, biopsy, and radiofrequency ablation, particularly for liver tumors. Employing image fusion technology enables the acquisition of real-time anatomical images overlayed with functional images of the same plane, thereby enhancing the diagnosis and treatment of liver cancers. This study provides a comprehensive examination of the fundamental concepts of image fusion technology, its application in tumor therapies, specifically for liver cancers. It finishes with an analysis of the limitations and future prospects of this technology [107].

6. IMAGE QUALITY METRICS IN MEDICAL IMAGE FUSION

The assessment of medical image fusion is crucial for verifying the efficacy of fusion algorithms. Image quality measures evaluate the visual integrity, information

retention, and diagnostic value of the fused image. These assessments are conducted utilizing either subjective or objective approaches [108, 109].

6.1. Subjective Evaluation

Subjective analysis entails expert evaluators who assess the images according to their visual characteristics, such as object clarity, spatial detail, geometric consistency, and color equilibrium. This method, although indicative of human perception, is compromised by observer bias, environmental reliance, and lack of reproducibility, rendering it less reliable for quantitative comparison.

6.2. Objective Evaluation

It utilizes the mathematical and statistical metrics to measure image quality quantitatively. These metrics yield reliable, quantifiable, and algorithm-independent outcomes, making them crucial for the consistent and automated validation of fusion approaches. They are further categorized into two categories such as those employing a reference image and those without a reference image, as depicted in Table 13, with each parameter demonstrating distinct characteristics. The objective image fusion performance characterization utilizing the gradient information is also taken into account. This provides an in-depth analysis by assessing total fusion performance, fusion loss, and fusion artifacts as represented in Table 14. It is noted that the total fusion performance is depicted by the sum of these three, and the result is unity, as shown in the formula [110-113].

7. EXPERIMENTAL SETUP AND DISCUSSION

In this section, a comprehensive evaluation of eight multimodal medical image fusion techniques, LEGFF, FGF-XDOG, MDHU, FDO-DPGF, CSMCA, S-ADE, PCLLE-NSCT, and NSST-AGPCNN, is conducted for dataset 1 [114] utilizing diverse quantitative criteria to evaluate information content, image quality, edge preservation, and noise reduction, and has been described in Table 15 along with mean and standard deviation. Of these evaluated approaches, LEGFF exhibited the highest entropy of 6.86 and average gradient of 7.06, signifying enhanced information richness and edge definition, while the mean entropy value is 6.44 ± 0.35 . CSMCA demonstrated superior image quality, attaining the highest PSNR (63.28) and the lowest MSE (0.0305), indicative of exceptional image reconstruction with minimum error. The spatial frequency values, which assess image detail, showed a moderate spread (17.79 ± 0.56), demonstrating that CSMCA and LEGFF retained excellent textural detail. In contrast, standard deviation results have revealed that LEGFF and S-ADE maintained a significant contrast. FGF-XDOG and S-ADE achieved the best visual information fidelity (VIF ~ 0.88), indicating superior perceptual quality. PCLLE-NSCT exhibited superior structural similarity, achieving a reduced spatial correlation difference (SCD = 1.72) compared to others. The Correlation Coefficient (CC) analysis indicated a preference for CSMCA and FDO-DPGF (CC ~ 0.698), emphasizing their robust correspondence with reference images.

Table 13. MMIF Metric with a reference image - definitions and interpretations.

Metric Name	Description	Formula / Expression	-
Average Pixel Intensity (API)	Measures image contrast by computing average intensity values.	$API = \bar{F} = \sum_{i=1}^M \sum_{j=1}^n f(i, j)$	[110, 111]
Standard Deviation (SD)	Measures the contrast or spread of the pixel intensity values around the mean intensity. A higher SD indicates more variation and, therefore, more detail and contrast.	$SD = \sqrt{\frac{\sum_{i=1}^M \sum_{j=1}^n (f(i, j) - F)^2}{mn}}$	[112]
Average Gradient (AG)	Evaluates the overall clarity and detail of the image by computing the average magnitude of the gradients in the image. To assess the sharpness and clarity of an image and quantify the overall contrast by measuring the rate of intensity change across adjacent pixels.	$AG = \frac{\sum_i \sum_j ((f(i, j) - f(i+1, j))^2 + (f(i, j) - f(i, j+1))^2)^{1/2}}{mn}$	[112]
Entropy (H)	Quantifies information content or randomness in the image. A higher entropy value indicates a richer and more complex image.	$H = - \sum_{k=0}^{255} p_k \log_2(p_k)$	[113]
Mutual Information (MI)	Assesses shared information between source and fused images. It should have a high value for better fusion.	$MI = MI_{AF} + MI_{BF}$	[110, 113]
Information Symmetry (FS)	Evaluates the symmetry of information between fused and input images.	$FS = 2 - \frac{MI_{AF}}{MI} - 0.5 $	[110]
Correlation Coefficient (CC)	It gives similarity in the small structures between the original and reconstructed images, where a higher value of correlation means more information is preserved. Determines the linear relationship between input and fused images.	$CC = (r_{AF} + r_{BF}) / 2$	[111]
Spatial Frequency (SF)	Measures the overall activity level or texture of an image, combining the row and column frequency components.	$SF = \sqrt{RF^2 + CF^2}$	[113]

Table 14. MMIF metric without a reference image - definitions and interpretations.

Metric Name	Description	Formula / Expression	Citations
Qab/f	Quantifies retained information from the source to the fused image.	$Qab/f + Lab/f + Nab/f = 1$	[110, 112]
Lab/f	Measures information loss during fusion.	$Qab/f + Lab/f + Nab/f = 1$	[110, 112]
Nab/f	Estimates artifacts or noise introduced after fusion.	$Qab/f + Lab/f + Nab/f = 1$	[110, 112]

Table 15. Quantitative Evaluation of various MMIF techniques on MRI and CT images for data set 1.

Technique →	LEGFF	FGF-XDOG	MDHU	FDO-DPGF	CSMCA	S-ADE	PCLLE-NSCT	NSST -AGPCNN	Mean± SD
Evaluation Parameter ↓									
EN	6.857	6.407	5.992	6.789	6.378	6.005	6.803	6.296	6.44 ± 0.35
SF	18.72	17.37	18.32	17.36	18.13	17.85	17.16	17.36	17.79 ± 0.56
SD	59.48	59.74	59.38	53.64	51.91	58.99	57.39	49.40	56.24 ± 4.03
PSNR	61.85	61.55	61.53	62.72	63.27	61.58	61.93	63.55	62.26 ± 0.82
MSE	0.0424	0.0454	0.0456	0.0347	0.0305	0.0451	0.0416	0.0321	0.04 ± 0.01
MI	3.046	4.710	5.854	3.074	2.328	5.795	3.291	1.489	3.70 ± 1.60
VIF	0.776	0.885	0.874	0.869	0.652	0.884	0.797	0.483	0.78 ± 0.14
AG	7.059	6.440	6.511	6.332	6.574	6.460	6.551	6.182	6.51 ± 0.25
CC	0.671	0.686	0.666	0.698	0.698	0.663	0.652	0.645	0.67 ± 0.02
SCD	1.823	1.898	1.841	1.766	1.746	1.831	1.724	1.453	1.76 ± 0.14
Qabf	0.731	0.774	0.778	0.771	0.654	0.776	0.739	0.600	0.73 ± 0.07
Nabf	0.018	0.021	0.024	0.012	0.020	0.027	0.025	0.018	0.02 ± 0.00

FGF-XDOG and MDHU attained the highest edge-based similarity (Qabf > 0.77), indicating efficient edge retention, which is essential in diagnostic imaging. FDO-DPGF demonstrated the lowest noise-based similarity (Nabf = 0.0126), indicating exceptional noise suppression. Mutual

Information (MI), crucial for evaluating modality complementarity, showed significant variance (mean = 3.7 ± 1.5), with MDHU and S-ADE outperforming. Visual Information Fidelity (VIF) and Qabf. NSST-AGPCNN and LEGFF regularly score well across most criteria, demonstrating

superior fusion quality. Future studies should provide larger datasets with repeated trials to allow for more rigorous statistical inferences.

The visual results in Fig. (16) also depict similar results where the source image (a) is a T1-weighted MRI image characterized by the dark appearance of cerebrospinal fluid and the high contrast between gray and white matter. CSF appears hypointense owing to the diminished signals on T1 T1-weighted sequence. T1-weighted scans offer superior anatomical detail and are commonly employed to evaluate brain morphology and the integrity of cerebral structures. The source image (b) is a non-contrast computed tomography scan of the brain, highlighting the bony content. CT scans are highly effective in identifying acute bleed, cerebral infarcts, fractures, and calcifications owing to their sensitivity to dense tissues such as bone. Bone exhibits hyper-density (white) because of elevated X-ray attenuation as compared to soft tissue. The images from (c) to (j) are the final fused images of these source images using the respective technique.

Table 16 provides an evaluation for dataset 2 [114], using the same set of techniques, and demonstrates diverse efficacy across essential quantitative parameters.

The average Entropy (EN) is 5.30 ± 0.09 , reflecting consistent information content with minimal variance. Spatial Frequency (SF), which is an indicator of textural detail, showed greater variation (20.38 ± 1.66), with LEGFF achieving the highest score (23.77), suggesting better edge detail retention.

Standard Deviation (SD) and PSNR were also stable, with PSNR averaging 68.44 ± 0.52 dB, indicating excellent noise suppression and fidelity. The Mean Square Error (MSE) values remained low (0.01 ± 0.00), reinforcing the high-quality reconstruction by all techniques, particularly NSST-AGPCNN (lowest MSE = 0.0074).

Mutual Information (MI) values showed moderate variance (3.87 ± 0.61), with S-ADE standing out as having the highest MI (4.976), highlighting its capacity to retain complementary modality features. VIF and CC metrics also revealed strong visual and structural correlation, particularly for FDO-DPGF and LEGFF. All techniques performed well with minor variability across metrics. Techniques like NSST-AGPCNN and S-ADE demonstrated superior balance in contrast enhancement, edge retention, and structural fidelity.

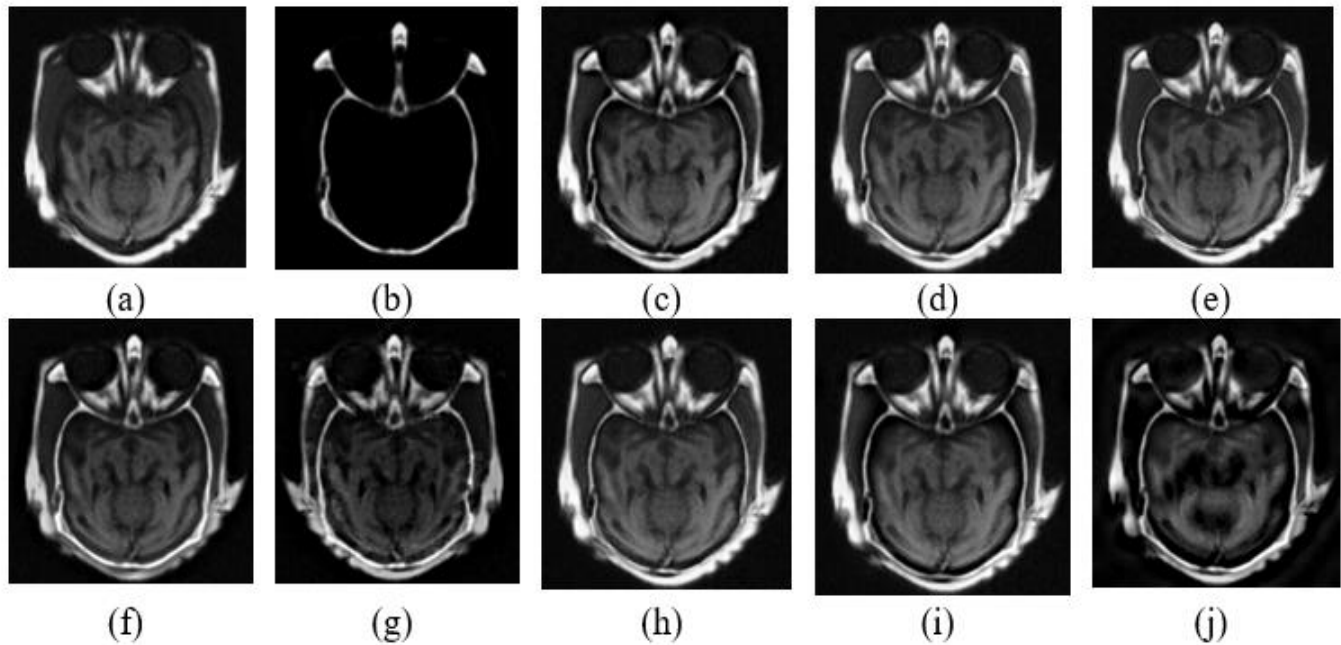


Fig. (16). Qualitative results for MRI/CT images. Dataset 1 (a) MRI image, (b) CT image, (c) LEGFF, (d) FGF-XDoG, (e) MDHU, (f) FDO-DPGF, (g) CSMCA, (h) S-ADE, (i) PCLLE NSCT, (j) NSST AGPCNN.

Table 16. Quantitative evaluation of various MMIF techniques on MRI and CT images for data set 2.

Technique →	LEGFF	FGF-XDOG	MDHU	FDO-DPGF	CSMCA	S-ADE	PCLLE-NSCT	NSST -AGPCNN	Mean ± SD
Evaluation Parameter ↓									
EN	5.336	5.322	5.210	5.262	5.426	5.317	5.382	5.161	5.30 ± 0.09
SF	23.77	20.43	20.40	18.12	20.20	20.13	18.91	21.07	20.38 ± 1.66
SD	61.97	62.11	61.12	57.59	56.33	61.59	58.77	55.31	59.35 ± 2.71
PSNR	68.36	68.26	68.01	68.24	68.82	67.76	68.63	69.42	68.44 ± 0.52
MSE	0.0094	0.0096	0.0102	0.0097	0.0085	0.0108	0.0088	0.0074	0.01 ± 0.00
MI	3.426	4.088	4.378	4.118	3.233	4.976	3.618	3.132	3.87 ± 0.63
VIF	0.577	0.594	0.625	0.870	0.528	0.682	0.625	0.517	0.63 ± 0.11
AG	6.397	5.580	5.212	4.723	5.754	5.355	5.348	5.681	5.51± 0.48
CC	0.926	0.927	0.914	0.903	0.914	0.910	0.919	0.923	0.92 ± 0.01
SCD	1.249	1.268	1.106	0.730	0.769	1.114	0.992	0.790	1.00 ± 0.22
Qabf	0.595	0.609	0.605	0.609	0.546	0.645	0.585	0.583	0.60 ± 0.03
Nabf	0.017	0.027	0.018	0.0153	0.028	0.006	0.035	0.0203	0.02 ± 0.01

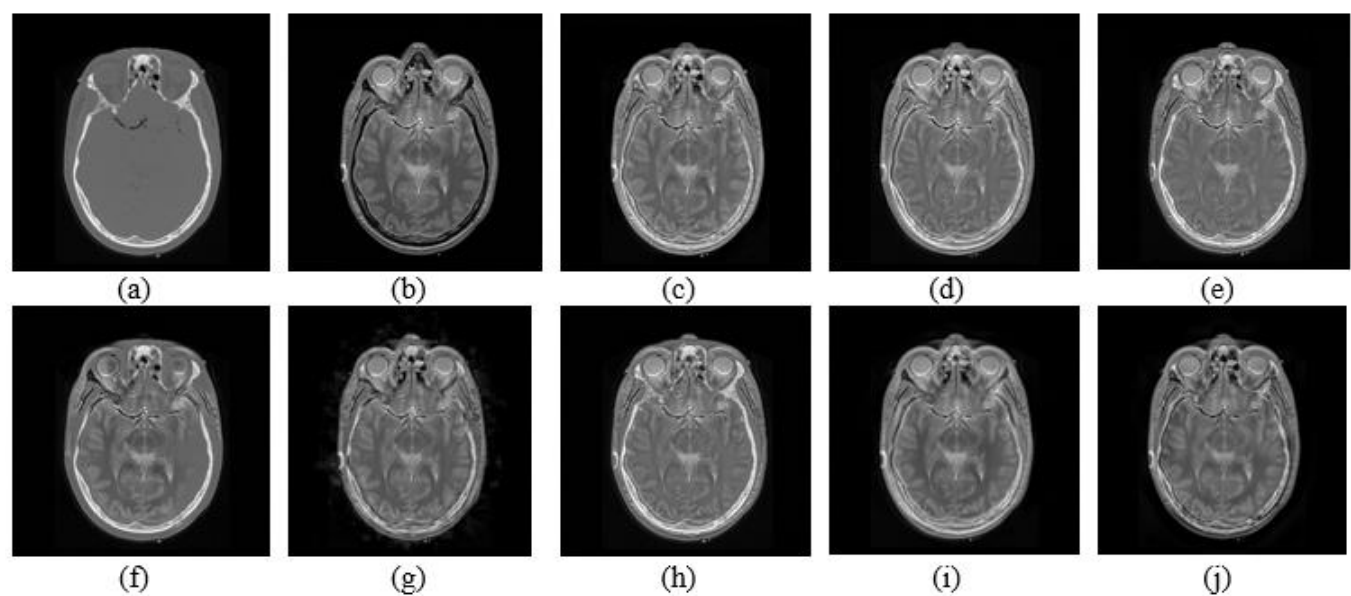


Fig. (17). Qualitative results for MRI/CT images Date set 2 (a) CT image, (b) MRI image, (c) LEGFF, (d) FGF-XDoG, (e) MDHU, (f) FDO-DPGF, (g) CSMCA, (h) S-ADE, (i) PCLLE NSCT, (j) NSST AGPCNN.

The visual results for dataset 2 are depicted in Fig. (17), where the source image (a) is a computed tomography scan of the brain proficient in assessing intracranial bleed and cerebral fractures. The image provides a clear depiction of the bone architecture with no evident indications of structural abnormalities. The source image (b) is a T2-weighted MRI scan of the brain, illustrating the differentiation of gray and White matter, and is marked by bright cerebrospinal fluid. The imaging modality is effective for identifying pathological alterations, including edema, demyelination, and infarctions. The images from (c) to (j) are the final fused images of these source images using the respective technique.

7.1. Research Trends in Modality Integration

The growing interest in MMIF studies from 2015 to 2024, analyzed according to the three most commonly used modality groups, MRI-PET, MRI-CT, and MRI-SPECT, is illustrated in Fig. (18). MRI-PET fusions report the greatest number of publications, with a significant boost in 2021, representing high influence in oncology and neuroimaging. The constant growth of MRI-CT literature (although its volume is less compared to MRI-PET) indicates growing use for surgical planning, and tasks where both soft and hard tissue information is needed.

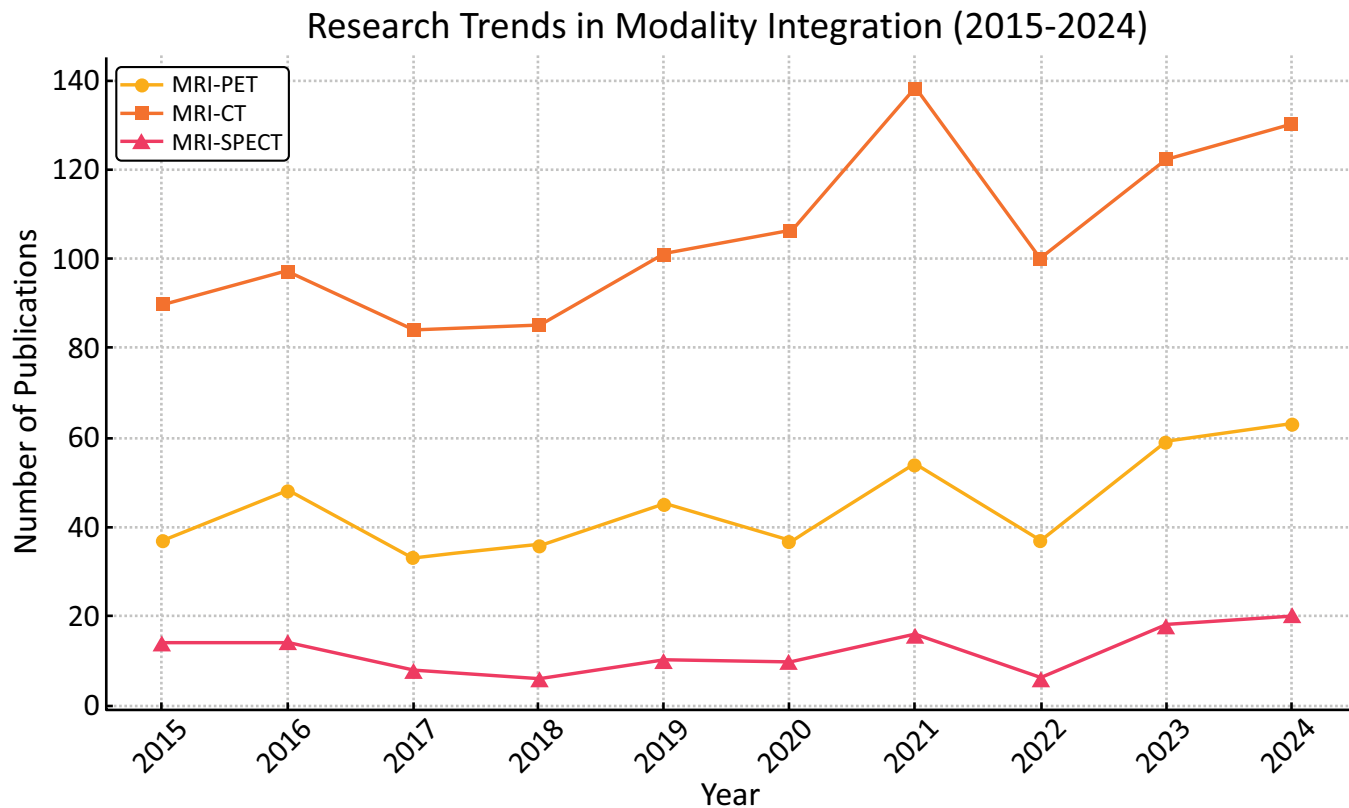


Fig. (18). Research Trend according to multi-modality combinations (WOS).

The MRI-SPECT fusion approach is the least discussed, possibly due to the lower spatial resolution and the comparatively narrower use of SPECT compared to PET. The possible correlation of periodic changes in MRI-PET and MRI-CT domains with the emergence of new advances, such as convolutional neural networks or transformer models, indicates that these improvements have likely reinforced the fusion and registration processes. The data shows an increasing interest in hybrid imaging as the main research topic, highlighting the clinical necessity for accurate diagnostics based on the integration of complementary modalities.

8. KEY CHALLENGES AND LIMITATIONS

8.1. Data Scarcity and Imbalance in Public Datasets

The foundation of any robust MMIF model is a sufficiently large and diverse dataset. However, available multimodal image datasets such as AANLIB, ADNI, TCIA, and MIDAS lack balance in organ representation, modality pairing, and demographic diversity. While these repositories provide aligned pairs (*e.g.*, MRI-PET), they often suffer from incomplete labeling and variation in acquisition protocols. For example, Venkatesan *et al.* [15] emphasized that most fusion research focuses on brain datasets (MRI-CT), leaving thoracic, abdominal, and musculoskeletal fusions underrepresented. The imbalance leads to biased models that cannot generalize across

anatomical regions. Moreover, annotating multimodal images, particularly PET and SPECT, requires domain expertise and is cost-intensive, limiting supervised learning approaches. Recent works, such as those by Tirupal *et al.* [8], propose the use of fuzzy sets and unsupervised learning to overcome the lack of labels, while Dinh [94, 95] explores decomposition techniques to create proxy supervision.

8.2. Registration and Inter-modality Inconsistency

Accurate registration is pivotal in MMIF, as misalignment between modalities can propagate errors into every subsequent fusion stage. Unlike unimodal registration, where intensity similarities guide optimization, multimodal images exhibit diverse characteristics (*e.g.*, CT for density, MRI for soft tissues, PET for metabolism), making intensity-based alignment ineffective. Errors in registration introduce artifacts, structural shifts, and contrast mismatches, especially at organ boundaries. Goyal *et al.* [90] and Ibrahim *et al.* [109] report that deformable and affine transformations often underperform when the inter-modality gap is large, such as in PET-MRI or SPECT-CT fusion. Furthermore, hybrid methods that employ wavelet or Laplacian transforms are highly sensitive to minor misregistrations, causing blur or duplication of anatomical features. Although deep-learning-based spatial transformers, such as the Swin Transformer by Ghosh [71], offer improved alignment, these solutions are

computationally expensive and poorly validated across multiple organs. Thus, the modality inconsistency and lack of robust, generalized registration algorithms significantly hinder the clinical reliability of MMIF systems.

8.3. Computational Overhead in Deep Learning-based MMIF

While Deep Learning (DL) methods, particularly CNNs, GANs, and U-Nets, have revolutionized image fusion, they bring substantial computational burdens. Training these models requires massive datasets, high-end GPUs, and time-intensive tuning. Liu *et al.* and Zhang *et al.* [60, 61] showed that deep CNNs produce sharper and semantically richer fused images, but the cost of training (over 20 million parameters) and risk of overfitting persist. These limitations restrict the practical deployment of MMIF in real-time or edge-based medical devices like portable ultrasound or emergency CT units. Efforts to develop lightweight architectures, such as Mobile Net or efficient transformer hybrids, have been partially successful. For instance, Kalamkar & Geetha [89] propose transfer learning-based MMIF using pretrained models to reduce training time. However, performance degradation and sensitivity to modality shifts are still major issues. Hybrid DL models, such as PCNN + NSCT or GANs over NSST coefficients, further increase architectural complexity, which limits scalability and increases latency during clinical inference.

8.4. Ethical and Privacy Concerns in Multimodal Data Use

The use of medical images, especially in a multimodal and longitudinal context, raises significant privacy and ethical issues. Most MMIF datasets are derived from patients with chronic or terminal conditions, making de-identification difficult due to unique anatomical signatures (*e.g.*, tumors or prostheses). Compliance with GDPR, HIPAA, and institutional IRB guidelines restricts dataset sharing. El-Shafai *et al.* [70] observed that fewer than 20% of fusion studies in recent years could access external datasets, limiting generalizability and leading to model bias. Federated learning, as explored in Goyal *et al.* [90], is a promising avenue to train models across silos without data exchange. However, challenges in harmonizing modalities, synchronizing update cycles, and addressing vulnerability to gradient attacks remain. Ethically, there's a lack of transparency in fusion models. Black-box CNNs may produce composite images that suppress or misrepresent subtle pathologies. There are also legal uncertainties in attributing diagnostic responsibility when AI-generated fusion images are used clinically. To address this, future MMIF research must include explainable AI (XAI) methods, probabilistic uncertainty maps, and formal ethical frameworks that define accountability for AI-assisted diagnostics [115]. While the field of MMIF continues to evolve rapidly, these four key challenges, data imbalance, registration inconsistency, computational overhead, and ethical constraints, remain persistent obstacles. Addressing these will require interdisciplinary collaboration between data scientists, radiologists,

ethicists, and software engineers. The integration of robust registration models, edge-efficient architectures, federated training schemes, and ethically compliant data pipelines will be vital to unlocking MMIF's full potential.

9. FUTURE RESEARCH DIRECTIONS IN MULTIMODAL MEDICAL IMAGE FUSION

9.1. Explainable AI (XAI) in MMIF

Explainable artificial intelligence is a technique for AI-powered diagnosis and analysis that ensures features such as ethics, transparency, and accountability in the traditional approach to AI. This will lead to outcome tracing and model improvements in health care. EXAI relies on feature extraction to make the model more explainable and interpretable. EXAI proposed a self-explanatory framework based on design principles for understanding and predicting the behavior of ML/DL models. Although deep models such as CNNs and Transformers outperform traditional algorithms, their "black-box" nature hinders clinical trust. Recent work integrates attention maps, Layer-wise Relevance Propagation (LRP), and Grad-CAMs into MMIF pipelines, allowing radiologists to verify the influence of fused features during diagnostics [115, 116].

9.2. Quantum Image Fusion

Quantum computation in medical image processing has improved edge detection, segmentation, watermarking, encryption, and classification. A quantum edge detection technique using superposition and fuzzy entropy can better detect strong and weak edges. Automatic hippocampal segmentation using a Quantum-Inspired Evolutionary Algorithm (QIEA) yielded good correlation between segmented and microscopic images. A hybrid technique using QPSO and fuzzy k-nearest neighbours enhances cervical cancer cell classification on the Herlev dataset for feature selection and classification. The hybrid method decreased features from 17 to 7, outperforming Naive Bayes and SVM with a 2% to 11% increase in accuracy. These inventions show how quantum computing might improve medical image analysis and diagnosis precision [117].

9.3. Federated and Privacy-preserving MMIF

Machine learning algorithms learn to solve problems autonomously based on the data provided to them, but they require extensive training to do so. Personal data in training datasets for AI systems, especially for health care applications, must be considered. Data from special categories (including health data) requires more safeguards than common data under the General Data Protection Regulation (GDPR). AI developers and users in health care are especially affected by this issue. With increasing data privacy regulations (*e.g.*, GDPR, HIPAA), centralized MMIF training on patient data faces ethical and legal barriers. Federated learning frameworks (*e.g.*, FL-MedFuseNet) enable MMIF model training across distributed hospital nodes without sharing raw data. This decentralized approach preserves privacy and supports continual learning from real-world clinical inputs [118].

9.4. Robotic Surgery and Smart Operating Rooms

The integration of MMIF into AI-assisted robotic surgeries is a fast-growing field. As the population ages, the prevalence of spinal degenerative illnesses such as lumbar disc herniation and spinal stenosis increases the need for accurate and safe spinal operations. The spine intricacy makes surgery difficult, making robotic help invaluable. Pedicle screw implantation is performed using surgical robots like TiRobot, Mazor, Da Vinci, ROSA, Excelsius GPS, and Orthobot, which enhance precision, reduce operative time, decrease the chances of hemorrhage, and minimize radiation exposure. These approaches use unimodal CT scans, which cannot detect nerves and intervertebral discs. The incorporation of a multimodal image fusion (CT/MR)- based software system for intraoperative navigation expands the horizons of robotic spinal surgery. Intuitive Surgical's Da Vinci system already shows early adoption of MMIF-enhanced visual pipelines, although this is mostly experimental. Future research could focus on ultra-low-latency hardware-driven MMIF solutions embedded into surgical robots. NVIDIA's Clara, a GPU-accelerated platform, is used to segment and diagnose cardiac images in real time. To improve processing speed and accuracy, the system takes advantage of powerful DL algorithms explicitly designed for cardiac imaging. Using rigorous data processing and a deep learning model, it can perform exact partitioning of cardiac components and identify positioning defects, resulting in the diagnosis of rapid heart arrhythmia [119, 120].

9.5. MMIF-based Watermarking for Tele-health Applications

Watermarking in medical image fusion involves embedding a hidden signal (such as patient ID, diagnosis detail, time stamps, or institutional information) into a fused image generated from multiple modalities. This ensures data integrity, ownership authentication, and secure communication in telemedicine or cloud environments. Embedding of watermark is done by techniques like Redundant Discrete Wavelet Transform (RDWT), Singular Value Decomposition (SVD), or NSCT. The integration of deep learning needs further exploration to create adaptive and intelligent watermarking methods [121].

CONCLUSION

This comprehensive review concludes that multimodal medical image fusion (MMIF) is a growing field with applications and modern techniques that allow the proper use of all available information, thus contributing to the improvement of clinical diagnostics. Firstly, the limitations of unimodal imaging were established, and the clinical need for combining MRI, CT, PET, and SPECT was explored. Combining strengths in each modality (by way of fusion) offers synergistic improvements to their diagnostic capability while addressing the limitations that each modality suffers from individually. The mentioned approaches, spatial and frequency-based fusion methods such as PCA, DWT, and NSCT, have proved useful in many early-stage applications owing to their simplicity and speed.

They are sensitive to noise and often suffer from issues like edge blurring or spectral distortion. This led to the development of more advance strategies like sparse representation, which is more flexible, particularly under uncertain and noisy imaging conditions. Additionally, when applicable with multi-scale transforms, sparse coding improves edge structure and clarity that is necessary for tumor detection and neurodegenerative diseases. With the introduction of Deep Learning (DL) and hybrid fusion models in the field, a paradigm shift has occurred, drastically improving fusion accuracy and robustness. It is effectuated by various architectures such as CNNs, U-Nets, GANs, Swin Transformers, *etc.* Deep Learning has brought its weaknesses along, but it has also brought hybrid models that blend Deep Learning with usual domains to minimize and compensate for their respective weak points. Moreover, high-quality datasets (TCIA, ADNI, OASIS, AANLIB) and evaluation metrics (SSIM, MI, and entropy) are used as a standard benchmark for MMIF models. The results of experiments across two datasets in this review highlight the effectiveness of hybrid and deep learning-based approaches. Yet, there are still many outstanding issues. Finding its way into clinical practice is impeded by data scarcity, registration inconsistencies, the computational cost of DL models, and the ethical use of necessary patient data. The promising emerging topics of interest included federated learning, explainable AI, quantum fusion, and watermarking in telemedicine. The integration of MMIF into surgical robotics is another frontier that needs to be explored. Finally, the findings of this review offer a fundamental analytical lens with which healthcare professionals, AI researchers, and developers of MMIF systems can improve the clinical scalability, interpretability, and ethics of the systems that are generated. It can be concluded that the field is rapidly evolving and holds promise for improving clinical decision-making. MMIF had demonstrated enhanced diagnostic accuracy by combining information from multiple sources, improved treatment planning, and even direct benefits to patients through shorter and safer procedures. MMIF offers immense potential yet has limitations like registration errors, computational burdens, generation of artifacts, loss of specific information, and a lack of standardized evaluation metrics. Ultimately, ongoing interdisciplinary collaborations will significantly enhance precision and accuracy, improving patient outcomes in the years to come.

AUTHORS' CONTRIBUTIONS

The authors confirm their contribution to the paper as follows: A.D.: Analysis and interpretation of results; S.B., B.G.: Writing - Reviewing and editing; N.G.: Writing - Original draft preparation. All authors reviewed the results and approved the final version of the manuscript.

LIST OF ABBREVIATIONS

MMIF	= Multimodal Medical Image Fusion
MRI	= Magnetic Resonance Imaging
CT	= Computed Tomography
PET	= Positron Emission Tomography

SPECT	= Single Photon Emission Computed Tomography
fMRI	= Functional Magnetic Resonance Imaging
CBCT	= Cone Beam Computed Tomography
CAD	= Computer-Aided Diagnosis
TCIA	= The Cancer Imaging Archive
OASIS	= Open Access Series of Imaging Studies
ADNI	= Alzheimer's Disease Neuroimaging Initiative
MIDAS	= Medical Image Data Archive System
AANLIB	= Annotated Alzheimer Neuroimaging Library
DDSM	= Digital Database for Screening Mammography
FLAIR	= Fluid-Attenuated Inversion Recovery
CSF	= Cerebrospinal Fluid
API	= Average Pixel Intensity
SD	= Standard Deviation
AG	= Average Gradient
EN	= Entropy
MI	= Mutual Information
FS	= Information Symmetry
CC	= Correlation Coefficient
SF	= Spatial Frequency
PSNR	= Peak Signal-to-Noise Ratio
MSE	= Mean Squared Error
SSIM	= Structural Similarity Index
VIF	= Visual Information Fidelity
SCD	= Spatial Correlation Difference
Qabf	= Edge-Based Similarity Measure
Nabf	= Noise-Based Similarity Measure
PCA	= Principal Component Analysis
ICA	= Independent Component Analysis
IHS	= Intensity-Hue-Saturation
DWT	= Discrete Wavelet Transform
NSCT	= Non-Subsampled Contourlet Transform
NSST	= Non-Subsampled Shearlet Transform
DFRWT	= Discrete Fractional Wavelet Transform
CSR	= Convolutional Sparse Representation
JSR	= Joint Sparse Representation
MCA	= Morphological Component Analysis
CS-MCA	= Convolutional Sparse Morphological Component Analysis
CNN	= Convolutional Neural Network
GAN	= Generative Adversarial Network

U-Net	= U-shaped Convolutional Neural Network
PCNN	= Pulse-Coupled Neural Network
ANFIS	= Adaptive Neuro-Fuzzy Inference System
IST	= Improved Structure Tensor
VMD	= Variational Mode Decomposition

CONSENT FOR PUBLICATION

Not applicable.

AVAILABILITY OF DATA AND MATERIALS

Authors may deposit their datasets openly to Zenodo Repository, in addition to their own or their institutional archives [114]. For more details please visit <https://openneuroimagingjournal.com/>

FUNDING

None.

CONFLICT OF INTEREST

Dr. Ayush Dogra is the Editorial Advisory Board of The Open Neuroimaging Journal.

ACKNOWLEDGEMENTS

Declared none.

REFERENCES

- [1] James AP, Dasarathy BV. Medical image fusion: A survey of the state of the art. *Inf Fusion* 2014; 19: 4-19. <http://dx.doi.org/10.1016/j.inffus.2013.12.002>
- [2] Kalamkar S, A GM. Multimodal image fusion: A systematic review. *Decision Analytics J* 2023; 9: 100327. <http://dx.doi.org/10.1016/j.dajour.2023.100327>
- [3] Zhang H, Xu H, Tian X, Jiang J, Ma J. Image fusion meets deep learning: A survey and perspective. *Inf Fusion* 2021; 76: 323-36. <http://dx.doi.org/10.1016/j.inffus.2021.06.008>
- [4] Li Y, Zhao J, Lv Z, Li J. Medical image fusion method by deep learning. *Int J Cognitiv Comput Engg* 2021; 2: 21-9. <http://dx.doi.org/10.1016/j.ijcce.2020.12.004>
- [5] Haribabu M, Guruviah V, Yogarajah P. Recent advancements in multimodal medical image fusion techniques for better diagnosis: An overview. *Curr Med Imaging* 2023; 19(7): 673-94. PMID: 35670346
- [6] Saleh MA, Ali AA, Ahmed K, Sarhan AM. A brief analysis of multimodal medical image fusion techniques. *Electronics* 2022; 12(1): 97. <http://dx.doi.org/10.3390/electronics12010097>
- [7] Bavirisetti DP, Kollu V, Gang X, Dhuli R. Fusion of MRI and CT images using guided image filter and image statistics. *Int J Imaging Syst Technol* 2017; 27(3): 227-37. <http://dx.doi.org/10.1002/ima.22228>
- [8] Tirupal T, Pandurangaiah Y, Roy A, Kishore VV, Nayyar A. On the use of UDWT and fuzzy sets for medical image fusion. *Multimedia Tools Appl* 2023; 83(13): 39647-75. <http://dx.doi.org/10.1007/s11042-023-16892-8>
- [9] Clark K, Vendt B, Smith K, et al. The Cancer Imaging Archive (TCIA): Maintaining and operating a public information repository. *J Digit Imaging* 2013; 26(6): 1045-57. <http://dx.doi.org/10.1007/s10278-013-9622-7> PMID: 23884657
- [10] Marcus DS, Wang TH, Parker J, Csernansky JG, Morris JC, Buckner RL. Open Access Series of Imaging Studies (OASIS): Cross-sectional MRI data in young, middle aged, nondemented, and demented older adults. *J Cogn Neurosci* 2007; 19(9): 1498-507.

- <http://dx.doi.org/10.1162/jocn.2007.19.9.1498> PMID: 17714011
- [11] Weiner MW, Veitch DP, Aisen PS, *et al.* The Alzheimer's disease neuroimaging initiative: A review of papers published since its inception. *Alzheimers Dement* 2013; 9(5): e111-94.
<http://dx.doi.org/10.1016/j.jalz.2013.05.1769> PMID: 23932184
 - [12] Advancing data science and AI. 2025. Available from: University of Michigan. <https://midas.umich.edu/>
 - [13] Heath M, Bowyer K, Kopans D, *et al.* Current status of the digital database for screening mammography. *Digital Mammography*. Springer 1998.
http://dx.doi.org/10.1007/978-94-011-5318-8_75
 - [14] Johnson KA, Becker JA. The whole brain atlas. 2025. Available from: <https://www.med.harvard.edu/aanlib/>
 - [15] Venkatesan B, Ragupathy US, Natarajan I. A review on multimodal medical image fusion towards future research. *Multimedia Tools Appl* 2023; 82(5): 7361-82.
<http://dx.doi.org/10.1007/s11042-022-13691-5>
 - [16] Indira KP, Rani Hemamalini R, Indhumathi R. Pixel based medical image fusion techniques using discrete wavelet transform and stationary wavelet transform. *Indian J Sci Technol* 2015; 8 (26).
<http://dx.doi.org/10.17485/ijst/2015/v8i26/56192>
 - [17] Ghassemian H. A review of remote sensing image fusion methods. *Inf Fusion* 2016; 32: 75-89.
<http://dx.doi.org/10.1016/j.inffus.2016.03.003>
 - [18] Huang B, Yang F, Yin M, Mo X, Zhong C. Computational and mathematical methods in medicine. Wiley 2017.
 - [19] Ullah Khan S, Ahmad Khan M, Azhar M, Khan F, Lee Y, Javed M. Multimodal medical image fusion towards future research: A review. *J King Saud Univ Comput Inform Sci* 2023; 35(8): 101733.
<http://dx.doi.org/10.1016/j.jksuci.2023.101733>
 - [20] Baraiya S, Gagnani LP. An introduction to image fusion techniques. *Int J Innov Res Sci Technol* 2014; 1(7): 86-9.
 - [21] Parekh P, Patel N, Macwan R, Prajapati P, Visavalia S. Comparative study and analysis of medical image fusion techniques. *Int J Computer Appl* 2014; 90(19): 12-6.
<http://dx.doi.org/10.5120/15827-4496>
 - [22] Morris C, Rajesh RS. Modified primitive image fusion techniques for the spatial domain. *Informatologia* 2015; 48(1-2): 71-7.
 - [23] Balachander B, Dhanasekaran D. Comparative study of image fusion techniques in spatial and transform domain. *ARPN J Eng Appl Sci* 2016; 11: 5779-83.
 - [24] Li W, Zhao Z, Du J, Wang Y. Edge-preserve filter image enhancement with application to MI fusion. *J Med Imaging Health Inform* 2017; 7(1): 16-24.
<http://dx.doi.org/10.1166/jmihi.2017.1980>
 - [25] Du J, Li W, Xiao B. Anatomical-functional image fusion by information of interest in local Laplacian filtering domain. *IEEE Trans Image Process* 2017; 26(12): 5855-66.
<http://dx.doi.org/10.1109/TIP.2017.2745202> PMID: 28858799
 - [26] Zhan K, Xie Y, Wang H, Min Y. Fast filtering image fusion. *J Electron Imaging* 2017; 26(6): 063004.
<http://dx.doi.org/10.1117/1.JEI.26.6.063004>
 - [27] Kotian SM, D'souza S, Gadagkar AV. A review on different techniques for medical image fusion. *International Journal of Recent Trends in Engineering & Research (IJRTER)* 2017; 3(11) November - 2017 (ISSN: 2455-1457)
<http://dx.doi.org/10.23883/IJRTER.2017.3507.QRVAL>
 - [28] Liu X, Mei W, Du H. Detail-enhanced multimodality medical image fusion based on gradient minimization smoothing filter and shearing filter. *Med Biol Eng Comput* 2018; 56(9): 1565-78.
<http://dx.doi.org/10.1007/s11517-018-1796-1> PMID: 29435706
 - [29] Na Y, Zhao L, Yang Y, Ren M. Guided filter-based images fusion algorithm for CT and MRI medical images. *IET Image Process* 2018; 12(1): 138-48.
<http://dx.doi.org/10.1049/iet-ivr.2016.0920>
 - [30] Saboori A, Birjandtalab J. PET-MRI image fusion using adaptive filter based on spectral and spatial discrepancy. *Signal Image Video Process* 2019; 13(1): 135-43.
<http://dx.doi.org/10.1007/s11760-018-1338-1>
 - [31] Pei C, Fan K, Wang W. Two-scale multimodal MI fusion based on guided filtering and sparse representation. *IEEE Access* 2020; 8: 140216-33.
<http://dx.doi.org/10.1109/ACCESS.2020.3013027>
 - [32] Tan W, Thitøn W, Xiang P, Zhou H. Multi-modal brain image fusion based on multi-level edge-preserving filtering. *Biomed Signal Process Control* 2021; 64: 102280.
<http://dx.doi.org/10.1016/j.bspc.2020.102280>
 - [33] Chen J, Zhang L, Lu L, Li Q, Hu M, Yang X. A novel medical image fusion method based on Rolling Guidance Filtering. *Internet of Things* 2021; 14: 100172.
<http://dx.doi.org/10.1016/j.iot.2020.100172>
 - [34] Sale D. An enhanced image fusion in the spatial domain based on modified independent component analysis. *Multimedia Tools Appl* 2022; 81(30): 44123-40.
<http://dx.doi.org/10.1007/s11042-022-13238-8>
 - [35] Kong W, Miao Q, Liu R, Lei Y, Cui J, Xie Q. Multimodal medical image fusion using gradient domain guided filter random walk and side window filtering in framelet domain. *Inf Sci* 2022; 585: 418-40.
<http://dx.doi.org/10.1016/j.ins.2021.11.033>
 - [36] Li J, Han D, Wang X, Yi P, Yan L, Li X. Multi-sensor medical-image fusion technique based on embedding bilateral filter in least squares and salient detection. *Sensors* 2023; 23(7): 3490.
<http://dx.doi.org/10.3390/s23073490> PMID: 37050552
 - [37] Feng Y, Wu J, Hu X, *et al.* Medical image fusion using bilateral texture filtering. *Biomed Signal Process Control* 2023; 85: 105004.
<http://dx.doi.org/10.1016/j.bspc.2023.105004>
 - [38] Zhang Y, Wang M, Xia X, *et al.* Medical image fusion based on quasi-cross bilateral filtering. *Biomed Signal Process Control* 2023; 80: 104259.
<http://dx.doi.org/10.1016/j.bspc.2022.104259>
 - [39] Singh R, Khare A. Fusion of multimodal medical images using Daubechies complex wavelet transform: A multiresolution approach. *Inf Fusion* 2014; 19: 49-60.
<http://dx.doi.org/10.1016/j.inffus.2012.09.005>
 - [40] Ganasala P, Prasad AD. Medical image fusion based on laws of texture energy measures in stationary wavelet transform domain. *Int J Imaging Syst Technol* 2020; 30(3): 544-57.
<http://dx.doi.org/10.1002/ima.22393>
 - [41] Bhateja V, Patel H, Krishn A, Sahu A, Lay-Ekuakille A. Multimodal MI sensor fusion framework using a cascade of wavelet and contourlet transform domains. *IEEE Sens J* 2015; 15(12): 6783-90.
<http://dx.doi.org/10.1109/JSEN.2015.2465935>
 - [42] Srivastava R, Prakash O, Khare A. Local energy-based multimodal medical image fusion in curvelet domain. *IET Comput Vis* 2016; 10(6): 513-27.
<http://dx.doi.org/10.1049/iet-cvi.2015.0251>
 - [43] Xu X, Wang Y, Chen S. Medical image fusion using discrete fractional wavelet transform. *Biomed Signal Process Control* 2016; 27: 103-11.
<http://dx.doi.org/10.1016/j.bspc.2016.02.008>
 - [44] Gomathi PS, Kalaavathi B. Multimodal MI fusion in non-subsampled contourlet transform domain. *Circuits and Systems* 2016; 7(8): 1598-610.
<http://dx.doi.org/10.4236/cs.2016.78139>
 - [45] Liu X, Mei W, Du H. Multi-modality medical image fusion based on image decomposition framework and nonsubsampled shearlet transform. *Biomed Signal Process Control* 2018; 40: 343-50.
<http://dx.doi.org/10.1016/j.bspc.2017.10.001>
 - [46] Gambhir D, Manchanda M. Waveatom transform-based multimodal medical image fusion. *Signal Image Video Process* 2019; 13(2): 321-9.
<http://dx.doi.org/10.1007/s11760-018-1360-3>
 - [47] Li L, Wang L, Wang Z, *et al.* A novel MI fusion approach based on nonsubsampled shearlet transform. *J Med Imaging Health Inform* 2019; 9(9): 1815-26.
<http://dx.doi.org/10.1166/jmihi.2019.2827>
 - [48] Ganasala P, Kumar V. CT and MR image fusion scheme in nonsubsampled contourlet transform domain. *J Digit Imaging*

- 2014; 27(3): 407-18.
<http://dx.doi.org/10.1007/s10278-013-9664-x> PMID: 24474580
- [49] Goyal B, Chyophel Lepcha D, Dogra A, Bhateja V, Lay-Ekuakille A. Measurement and analysis of multi-modal image fusion metrics based on structure awareness using domain transform filtering. *Measurement* 2021; 182: 109663.
<http://dx.doi.org/10.1016/j.measurement.2021.109663>
- [50] Khare A, Khare M, Srivastava R. Shearlet transform based technique for image fusion using median fusion rule. *Multimedia Tools Appl* 2021; 80(8): 11491-522.
<http://dx.doi.org/10.1007/s11042-020-10184-1>
- [51] Kong W, Li Y, Lei Y. MI fusion using SKWGF and SWF in the framelet transform domain. *Electronics* 2023; 12(12): 2659.
<http://dx.doi.org/10.3390/electronics12122659>
- [52] Diwakar M, Singh P, Ravi V, Maurya A. A non-conventional review on multi-modality-based medical image fusion. *Diagnostics* 2023; 13(5): 820.
<http://dx.doi.org/10.3390/diagnostics13050820> PMID: 36899965
- [53] Liu Y, Chen X, Liu A, Ward RK, Wang ZJ. Recent advances in sparse representation based medical image fusion. *IEEE Instrum Meas Mag* 2021; 24(2): 45-53.
<http://dx.doi.org/10.1109/MIM.2021.9400960>
- [54] Zhang Q, Fu Y, Li H, Zou J. Dictionary learning method for joint sparse representation-based image fusion. *Opt Eng* 2013; 52(5): 057006.
<http://dx.doi.org/10.1117/1.OE.52.5.057006>
- [55] Zong J, Qiu T. Medical image fusion based on sparse representation of classified image patches. *Biomed Signal Process Control* 2017; 34: 195-205.
<http://dx.doi.org/10.1016/j.bspc.2017.02.005>
- [56] Liu Y, Chen X, Cheng J, Peng H. A medical image fusion method based on convolutional neural networks. 2017 20th International Conference on Information Fusion (Fusion). Xi'an, China, 10-13 July 2017. pp. 1-7
<http://dx.doi.org/10.23919/ICIF.2017.8009769>
- [57] Liu Y, Chen X, Ward RK, Wang ZJ. Medical image fusion via convolutional sparsity based morphological component analysis. *IEEE Signal Process Lett* 2019; 26(3): 485-9.
<http://dx.doi.org/10.1109/LSP.2019.2895749>
- [58] Shabanzade F, Ghassemian H. Multimodal image fusion via sparse representation and clustering-based dictionary learning algorithm in nonsubsampled contourlet domain. *Proceedings of the 2016 8th International Symposium on Telecommunications (IST)*. Tehran, Iran, 2016; 472-7.
<http://dx.doi.org/10.1109/ISTEL.2016.7881866>
- [59] Hermessi H, Mourali O, Zagrouba E. Multimodal medical image fusion review: Theoretical background and recent advances. *Signal Processing* 2021; 183: 108036.
<http://dx.doi.org/10.1016/j.sigpro.2021.108036>
- [60] Liu Y, Liu S, Wang Z. A general framework for image fusion based on multi-scale transform and sparse representation. *Inf Fusion* 2015; 24: 147-64.
<http://dx.doi.org/10.1016/j.inffus.2014.09.004>
- [61] Zhang Q, Liu Y, Blum RS, Han J, Tao D. Sparse representation based multi-sensor image fusion for multi-focus and multi-modality images: A review. *Inf Fusion* 2018; 40: 57-75.
<http://dx.doi.org/10.1016/j.inffus.2017.05.006>
- [62] Yousif A S, Omar Z, Sheikh U U. An improved approach for medical image fusion using sparse representation and Siamese convolutional neural network. *Biomed Signal Process Control* 2022; 72: 103357.
<http://dx.doi.org/10.1016/j.bspc.2021.103357>
- [63] Liu Y, Chen X, Peng H, Wang Z. Multi-focus image fusion with a deep convolutional neural network. *Inf Fusion* 2017; 36: 191-207.
<http://dx.doi.org/10.1016/j.inffus.2016.12.001>
- [64] Gibson E, Li W, Sudre C, et al. NiftyNet: A deep-learning platform for medical imaging. *Comput Methods Programs Biomed* 2018; 158: 113-22.
<http://dx.doi.org/10.1016/j.cmpb.2018.01.025> PMID: 29544777
- [65] Xia K, Yin H, Wang J. A novel improved deep convolutional neural network model for medical image fusion. *Cluster Comput* 2019; 22(S1): 1515-27.
<http://dx.doi.org/10.1007/s10586-018-2026-1>
- [66] Wang K, Zheng M, Wei H, Qi G, Li Y. Multi-modality medical image fusion using convolutional neural network and contrast pyramid. *Sensors* 2020; 20(8): 2169.
<http://dx.doi.org/10.3390/s20082169> PMID: 32290472
- [67] Li Y, Zhao J, Lv Z, Pan Z. Multimodal medical supervised image fusion method by CNN. *Front Neurosci* 2021; 15: 638976.
<http://dx.doi.org/10.3389/fnins.2021.638976> PMID: 34149344
- [68] Chuang CH, Chang KY, Huang CS, Jung TP. IC-U-Net: A U-Net-based denoising autoencoder using mixtures of independent components for automatic EEG artifact removal. *Neuroimage* 2022; 263: 119586.
<http://dx.doi.org/10.1016/j.neuroimage.2022.119586> PMID: 36031182
- [69] Kumar M, Ranjan N, Chourasia B. Hybrid methods of contourlet transform and particle swarm optimization for multimodal MI fusion. 2021 International Conference on Artificial Intelligence and Smart Systems (ICAIS). Coimbatore, India, 2021. pp. 945-951.
<http://dx.doi.org/10.1109/ICAIS50930.2021.9396021>
- [70] El-Shafai W, Ghandour C, El-Rabaie S. Improving traditional method used for medical image fusion by deep learning approach-based convolution neural network. *J Opt* 2023; 52(4): 2253-63.
<http://dx.doi.org/10.1007/s12596-023-01123-y>
- [71] Ghosh TNJ. Performance analysis of multimodal MI fusion using AMT-DWT-based pre-processing and customized CNN for denoising. *Multimedia Tools Appl* 2024; 84(20): 22269-301.
- [72] Xia J, Chen Y, Chen A, Chen Y. Medical image fusion based on sparse representation and PCNN in NSCT Domain. *Comput Math Methods Med* 2018; 2018: 2806047.
<http://dx.doi.org/10.1155/2018/2806047> PMID: 29991960
- [73] Wang J, Li X, Zhang Y, Zhang X. Adaptive decomposition method for multi-modal medical image fusion. *IET Image Process* 2018; 12(8): 1403-12.
<http://dx.doi.org/10.1049/iet-ipr.2017.1067>
- [74] Bhateja V, Krishn A, Patel H, Sahu A. Medical image fusion in wavelet and ridgelet domains. *Int J Rough Sets Data Anal* 2015; 2(2): 78-91.
<http://dx.doi.org/10.4018/IJRSDA.2015070105>
- [75] Du J, Li W, Tan H. Intrinsic image decomposition-based grey and pseudo-color medical image fusion. *IEEE Access* 2019; 7: 56443-56.
<http://dx.doi.org/10.1109/ACCESS.2019.2900483>
- [76] Zhao F, Xu G, Zhao W. CT and MR image fusion based on adaptive structure decomposition. *IEEE Access* 2019; 7: 44002-9.
<http://dx.doi.org/10.1109/ACCESS.2019.2908378>
- [77] Maqsood S, Javed U. Multi-modal medical image fusion based on two-scale image decomposition and sparse representation. *Biomed Signal Process Control* 2020; 57: 101810.
<http://dx.doi.org/10.1016/j.bspc.2019.101810>
- [78] Wang Z, Cui Z, Zhu Y. Multi-modal medical image fusion by Laplacian pyramid and adaptive sparse representation. *Comput Biol Med* 2020; 123: 103823.
<http://dx.doi.org/10.1016/j.compbiomed.2020.103823> PMID: 32658780
- [79] Liu Y, Zhou D, Nie R, et al. Robust spiking cortical model and total-variational decomposition for multimodal medical image fusion. *Biomed Signal Process Control* 2020; 61: 101996.
<http://dx.doi.org/10.1016/j.bspc.2020.101996>
- [80] Yadav SP, Yadav S. Image fusion using hybrid methods in multimodality medical images. *Med Biol Eng Comput* 2020; 58(4): 669-87.
<http://dx.doi.org/10.1007/s11517-020-02136-6> PMID: 31993885
- [81] Ashwanth B, Swamy KV. Medical image fusion using transform techniques. 5th International Conference on Devices, Circuits, and Systems (ICDCS). Coimbatore, Tamil Nadu, India, 5-6 March 2020. pp. 303-306.
<http://dx.doi.org/10.1109/ICDCS48716.2020.243604>
- [82] Huang B, Yang F, Yin M, Mo X, Zhong C. A review of multimodal

- MI fusion techniques. *Comput Math Methods Med* 2020; 2020(1): 8279342.
PMID: 32377226
- [83] Kaur H, Kumar S, Behgal KS, Sharma Y, Multi-Modality MI. Multi-modality medical image fusion using cross-bilateral filter and neuro-fuzzy approach. *J Med Phys* 2021; 46(4): 263-77.
http://dx.doi.org/10.4103/jmp.JMP_14_21 PMID: 35261496
- [84] Kaur H, Koundal D, Kadyan V. Image fusion techniques: A survey. *Arch Comput Methods Eng* 2021; 28(7): 4425-47.
<http://dx.doi.org/10.1007/s11831-021-09540-7> PMID: 33519179
- [85] Polinati S, Bavirisetti DP, Rajesh KNPVS, Naik GR, Dhuli R. The fusion of MRI and CT medical images using variational mode decomposition. *Appl Sci* 2021; 11(22): 10975.
<http://dx.doi.org/10.3390/app112210975>
- [86] Li X, Zhou F, Tan H, Zhang W, Zhao C. Multimodal medical image fusion based on joint bilateral filter and local gradient energy. *Inf Sci* 2021; 569: 302-25.
<http://dx.doi.org/10.1016/j.ins.2021.04.052>
- [87] Zhu R, Li X, Zhang X, Wang J. HID: the hybrid image decomposition model for MRI and CT fusion. *IEEE J Biomed Health Inform* 2022; 26(2): 727-39.
<http://dx.doi.org/10.1109/JBHI.2021.3097374> PMID: 34270437
- [88] Alseelawi N, Hazim HT. A novel method of multimodal MI fusion based on hybrid approach of NSCT and DTCWT. *Int J Online Biomed Eng* 2022; 18(3): 114-33.
<http://dx.doi.org/10.3991/ijoe.v18i03.28011>
- [89] Kalamkar S, A GM, Multi-Modal MI. Multi-modal medical image fusion using transfer learning approach. *Int J Adv Comput Sci Appl* 2022; 13 (12).
<http://dx.doi.org/10.14569/IJACSA.2022.0131259>
- [90] Goyal B, Dogra A, Lepcha DC, *et al.* Multi-modality image fusion for medical assistive technology management based on hybrid domain filtering. *Expert Syst Appl* 2022; 209: 118283.
<http://dx.doi.org/10.1016/j.eswa.2022.118283>
- [91] Faragallah OS, El-Hoseny H, El-Shafai W, *et al.* Optimized multimodal MI fusion framework using multi-scale geometric and multi-resolution geometric analysis. *Multimedia Tools Appl* 2022; 81(10): 14379-401.
<http://dx.doi.org/10.1007/s11042-022-12260-0>
- [92] Zhou J, Xing X, Yan M, *et al.* A fusion algorithm based on composite decomposition for PET and MRI medical images. *Biomed Signal Process Control* 2022; 76: 103717.
<http://dx.doi.org/10.1016/j.bspc.2022.103717>
- [93] Kittusamy K, Shanmuga Vadivu Sampath Kumar L. Non Sub-Sampled Contourlet with Joint Sparse Representation Based Medical Image Fusion. *Comput Syst Sci Eng* 2023; 44(3): 1989-2005.
<http://dx.doi.org/10.32604/csse.2023.026501>
- [94] Dinh PH. Medical image fusion based on enhanced three-layer image decomposition and Chameleon swarm algorithm. *Biomed Signal Process Control* 2023; 84: 104740.
<http://dx.doi.org/10.1016/j.bspc.2023.104740>
- [95] Dinh PH. A novel approach using the local energy function and its variations for medical image fusion. *Imaging Sci J* 2023; 71(7): 660-76.
<http://dx.doi.org/10.1080/13682199.2023.2190947>
- [96] Balakrishna T, Hannan MA, Nimishka G. DWT-Based image fusion technique in matlab: Identifying the most effective method. *E3S Web Conf* 2023; 391: 01076.
- [97] Moghtaderi S, Einlou M, Wahid KA, Lukong KE. Advancing multimodal medical image fusion: An adaptive image decomposition approach based on multilevel Guided filtering. *R Soc Open Sci* 2024; 11(4): rsos.231762.
<http://dx.doi.org/10.1098/rsos.231762> PMID: 38601031
- [98] Zhao H, Zhang X, Wang Z, Yang F, Zhu R. Multi-modal medical image fusion via three-scale decomposition and structure similarity balanced optimization. *Biomed Signal Process Control* 2024; 95: 106358.
<http://dx.doi.org/10.1016/j.bspc.2024.106358>
- [99] Victor E. Magnetic resonance imaging-based synthetic computed tomography of the lumbar spine for surgical planning: A clinical proof-of-concept. *Neurosurg Focus* . 2021; 50(1): E13.
<http://dx.doi.org/10.3171/2020.10.FOCUS20801>
- [100] Haleem Abid. Role of CT and MRI in the design and development of orthopaedic model using additive manufacturing. *J Clin Orthop Trauma* 2021; 9(3): 213-7.
- [101] Bagaria V, Deshpande S, Rasalkar D D, Kuthe A, Paunipagar B K. Use of rapid prototyping and three-dimensional reconstruction modeling in the management of complex fractures. *Eur J Radiol* 2011; 80(3): 814-20.
<http://dx.doi.org/10.1016/j.ejrad.2010.10.007> PMID: 21256690
- [102] Jian Z, Li J, Wu K, *et al.* Surgical effects of resecting skull base tumors using pre-operative multimodal image fusion technology: A retrospective study. *Front Neurol* 2022; 13: 895638.
<http://dx.doi.org/10.3389/fneur.2022.895638> PMID: 35645981
- [103] Chen KT, Lin MHC, Tsai YH, Lee MH, Yang JT. Application of MRI and intraoperative CT fusion images with integrated neuronavigation in percutaneous radiofrequency trigeminal rhizotomy. *Acta Neurochir (Wien)* 2015; 157(8): 1443-8.
<http://dx.doi.org/10.1007/s00701-015-2459-8> PMID: 26066533
- [104] Vulpe H, Save AV, Xu Y, *et al.* Frameless stereotactic radiosurgery on the gamma knife icon: Early experience from 100 patients. *Neurosurgery* 2020; 86(4): 509-16.
<http://dx.doi.org/10.1093/neuros/nyz227> PMID: 31375826
- [105] Ahuja CK, Vyas S, Jani P, *et al.* Radiological parameters for gamma knife radiosurgery. *Neurol India* 2023; 71: S198-206.
<http://dx.doi.org/10.4103/0028-3886.373642> PMID: 37026353
- [106] Wang SY, Chen XX, Li Y, Zhang YY. Application of multimodality imaging fusion technology in diagnosis and treatment of malignant tumors under the precision medicine plan. *Chin Med J (Engl)* 2016; 129(24): 2991-7.
<http://dx.doi.org/10.4103/0366-6999.195467> PMID: 27958232
- [107] Li C, Zhu A. Application of image fusion in diagnosis and treatment of liver cancer. *Appl Sci* 2020; 10(3): 1171.
<http://dx.doi.org/10.3390/app10031171>
- [108] Meher B, Agrawal S, Panda R, Abraham A. A survey on region based image fusion methods. *Inf Fusion* 2019; 48: 119-32.
<http://dx.doi.org/10.1016/j.inffus.2018.07.010>
- [109] Ibrahim SI, Makhlof MA, El-Tawel GS. Multimodal medical image fusion algorithm based on pulse coupled neural networks and nonsubsampled contourlet transform. *Med Biol Eng Comput* 2023; 61(1): 155-77.
<http://dx.doi.org/10.1007/s11517-022-02697-8> PMID: 36342598
- [110] Goyal B, Dogra A, Khoond R, Chyophel Lepcha D, Goyal V. Medical image fusion based on anisotropic diffusion and non-subsampled contourlet transform. *Comput Mater Continua* 2023; 76(1): 311-27.
<http://dx.doi.org/10.32604/cmc.2023.038398>
- [111] Shreyamsha Kumar BK. Image fusion based on pixel significance using cross bilateral filter. *Signal Image Video Process* 2015; 9(5): 1193-204.
<http://dx.doi.org/10.1007/s11760-013-0556-9>
- [112] Li S, Kang X, Fang L, Hu J, Yin H. Pixel-level image fusion: A survey of the state of the art. *Inform Fusion* 2017; 33: 100.
- [113] Gao J, Li P, Chen Z, Zhang J. A survey on deep learning for multimodal data fusion. *Neural Comput* 2020; 32(5): 829-64.
http://dx.doi.org/10.1162/neco_a_01273 PMID: 32186998
- [114] MedFuse. 2026. Available from: <https://github.com/dawachyophel/medical-fusion/tree/main/MyDataset>
- [115] Saraswat D, Bhattacharya P, Verma A, *et al.* Explainable AI for healthcare 5.0: Opportunities and challenges. *IEEE Access* 2022; 10: 84486-517.
<http://dx.doi.org/10.1109/ACCESS.2022.3197671>
- [116] Mi J, Wang L, Liu Y, Zhang J. KDE-GAN: A multimodal medical image-fusion model based on knowledge distillation and explainable AI modules. *Comput Biol Med* 2022; 151(Pt A): 106273.
<http://dx.doi.org/10.1016/j.compbiomed.2022.106273> PMID: 36368109
- [117] Elaraby A. Quantum medical images processing foundations and

- applications. *IET Quantum Commun* 2022; 3(4): 201-13.
<http://dx.doi.org/10.1049/qtc2.12049>
- [118] Vota F, Pediconi F, Liscio A. Federated learning in healthcare: Addressing AI challenges and operational realities under the GDPR. *J Data Protect Privacy* 2025; 7(3): 235-51.
<http://dx.doi.org/10.69554/WSZT6624>
- [119] Navaneethan S, Hemanth G, Nikilkumar R. Leveraging nvidia clara for real-time cardiac image segmentation and diagnosis. 2024 International Conference on Innovative Computing, Intelligent Communication and Smart Electrical Systems (ICSSES). Chennai, India, 2024, pp. 1-7
<http://dx.doi.org/10.1109/ICSSES63760.2024.10910358>
- [120] Yuan S, Chen R, Zang L, *et al.* Development of a software system for surgical robots based on multimodal image fusion: Study protocol. *Front Surg* 2024; 11: 1389244.
<http://dx.doi.org/10.3389/fsurg.2024.1389244> PMID: 38903864
- [121] Singh KN, Singh OP, Singh AK, Agrawal AK. Watmif: Multimodal medical image fusion-based watermarking for telehealth applications. *Cognit Comput* 2022; 16(4): 1-17.
<http://dx.doi.org/10.1007/s12559-022-10040-4> PMID: 35818513